REPORT NO. NADC-88138-60
Contract No. N62269-85-C-0290

CORROSION INHIBITORS FOR METALS IN NAVAL ENVIRONMENTS

S. Hettiarachchi, E. J. Crawford, Y. W. Chan, D. Parish, L. L. Ackerman, and R. G. Wilson, Jr.
SRI INTERNATIONAL CHEMISTRY LABORATORY
333 Ravenswood Avenue
Menlo Park, CA 94025

15 JUNE 1988

FINAL REPORT
PERIOD COVERING 1985 TO 1988
Task No. WR22-01
Program Element No. 61153N

Approved for Public Release; Distribution is Unlimited

Prepared for
Air Vehicle and Crew Systems Technology Department (Code 6062)
NAVAL AIR DEVELOPMENT CENTER
Warminster, Pa 18974-5000

NOTICES

REPORT NUMBERING SYSTEM - The numbering of technical project reports issued by the Naval Air Development Center is arranged for specific identification purposes. Each number consists of the Center acronym, the calendar year in which the number was assigned, the sequence number of the report within the specific calandar year, and the official 2-digit correspondence code of the Command Officer or the Functional Department responsible for the report. For example: Report No. NADC 88020-60 indicates the twentieth Center report for the year 1988 and prepared by the Air Vehicle and Crew Systems Technology Department. The numerical codes are as follows:

CODE	OFFICE OR DEPARTMENT
00	Commander, Naval Air Development Center
01	Technical Director, Naval Air Development Center
05	Computer Department
10	AntiSubmarine Warfare Systems Department
20	Tactical Air Systems Department
30	Warfare Systems Analysis Department
40	Communication Navigation Technology Department
50	Mission Avionics Technology Department
60	Air Vehicle & Crew Systems Technology Department
70	Systems & Software Technology Department
80	Engineering Support Group
90	Test & Evaluation Group

PRODUCT ENDORSEMENT - The discussion or instructions concerning commercial products herein do not constitute an endorsement by the Government nor do they convey or imply the license or right to use such products.

Unclassified

SECURITY CLASSIFICATION OF THIS PAGE

REPORT DOCUMENTATION PAGE

Form Approved
OMB No. 0704-0188

1a REPORT SECURITY CLASSIFICATION Unclassified	1b RESTRICTIVE MARKINGS
2a SECURITY CLASSIFICATION AUTHORITY	3 DISTRIBUTION/AVAILABILITY OF REPORT Approved for Public Release, Distribution is Unlimited
2b DECLASSIFICATION/DOWNGRADING SCHEDULE	
4 PERFORMING ORGANIZATION REPORT NUMBER(S) Project 1178	5 MONITORING ORGANIZATION REPORT NUMBER(S) NADC-88138-60
6a NAME OF PERFORMING ORGANIZATION SRI International 6b OFFICE SYMBOL (*If applicable*)	7a NAME OF MONITORING ORGANIZATION Aircraft and Crew Systems Technology Department (Code 6062)
6c ADDRESS (*City, State, and ZIP Code*) Chemistry Laboratory 333 Ravenswood Avenue Menlo, CA 94025	7b ADDRESS (*City, State, and ZIP Code*) NAVAL AIR DEVELOPMENT CENTER Warminster, PA 18974-5000
8a NAME OF FUNDING/SPONSORING ORGANIZATION NAVAL AIR SYSTEMS COMMAND 8b OFFICE SYMBOL (*If applicable*) AIR-530	9 PROCUREMENT INSTRUMENT IDENTIFICATION NUMBER Contract No. N62269-85-C-0290
8c ADDRESS (*City, State, and ZIP Code*) DEPARTMENT OF THE NAVY Washington, DC 20361	10 SOURCE OF FUNDING NUMBERS PROGRAM ELEMENT NO: 61153N; PROJECT NO:; TASK NO: WR22-01; WORK UNIT ACCESSION NO:
11 TITLE (*Include Security Classification*) (U) Corrosion Inhibitors for Metals in Naval Environments	
12 PERSONAL AUTHOR(S) Hettiarachchi, S., Crawford, E.J., Chan, Y.W., Parish, D., Ackerman, L.L. and Wilson Jr., R.G.	
13a TYPE OF REPORT Final Report 13b TIME COVERED FROM 1985 TO 1988	14 DATE OF REPORT (*Year, Month, Day*) 1988 June 15 15 PAGE COUNT
16 SUPPLEMENTARY NOTATION	

17 COSATI CODES		
FIELD	GROUP	SUB-GROUP
11	03	

18 SUBJECT TERMS (*Continue on reverse if necessary and identify by block number*)
Macrocyclic Compounds; Phthalocyanines; Polymeric Phthalocyanines; Corrosion Inhibitors; Aluminum Alloys; Steels; Naval Environment; A.C. Impedance Analysis; Electrochemistry, corrosion Resistant Alloys, sea water corrosion (GS)

19 ABSTRACT (*Continue on reverse if necessary and identify by block number*)

Macrocyclic compounds, phthalocyanines, were studied as corrosion inhibitors for metals because of their ability to interact with the surface, their stability, and their rigid planarity. A synthetic approach was used to tailor-make a system to achieve best corrosion inhibition. The steps involved consisted of: (1) Synthesis of two types of water-soluble phthalocyanines - tertrasulfonated and tetraamino (quaternized) metallo-phthalocyanines. When tested in 1% NaCl at pH2, they were not very effective inhibitors. (2) Synthesis of polymeric phthalocyanines as corrosion inhibiting coatings - polymerization by decarboxylation of chloroiron (III) tetracarboxyphthalocyanine and reacting the acid chloride to attach 6 to 12 carbon alkyl chain. This showed corrosion inhibition efficiency of up to 88%. The effect of central metal ion into the phthalocyanine ring was most effective with long alkyl chanin Zn(II) material. The inhibition with the above system was limited to steels only and could not be effective on aluminum alloys. However, when aluminum surface was pre-treated with aminosilanes, The binding of the phthalocyanine improved significantly. Keywords: sodium chloride

20 DISTRIBUTION/AVAILABILITY OF ABSTRACT ☐ UNCLASSIFIED/UNLIMITED ☐ SAME AS RPT ☐ DTIC USERS	21 ABSTRACT SECURITY CLASSIFICATION Unclassified
22a NAME OF RESPONSIBLE INDIVIDUAL Dr. Vinod S. Agarwala	22b TELEPHONE (*Include Area Code*) (215) 441-1122 22c OFFICE SYMBOL Code 6062

DD Form 1473, JUN 86 *Previous editions are obsolete*

S/N 0102-LF-014-6603

SECURITY CLASSIFICATION OF THIS PAGE
UNCLASSIFIED

SUMMARY

SRI International undertook this project for the Naval Air Development Center (Contract No. N62269-85-C-0290) to develop macrocyclic corrosion inhibitors for metals in a naval environment. Phthalocyanines were relected because of their ability to chemisorb onto a surface effectively, their stability, and their rigid planarity.

The accomplishments of the project can be divided into three areas: (1) synthesis and testing of water-soluble phthalocyanines as corrosion inhibitors, (2) synthesis and testing of polymeric phthalocyanines as corrosion-inhibiting coatings, and (3) synthesis and testing of phthalocyanine derivatives with long-chain aliphatic substituents to provide an oily film on the metal surface that enhances corrosion inhibition.

We synthesized seven water-soluble phthalocyanines of two types, tetrasulfonated and tetraamino (quaternized): (1) cobalt(II) tetrasulfophthalocyanine [Co(II) TSPC], (2) hydroxycobalt(III) tetrasulfophthalocyanine [HOCo(III) TSPC], (3) iron(II) tetrasulfophthalocyanine [Fe(II) TSPC], (4) hydroxyiron(III) tetrasulfophthalocyanine [HOFe(III) TSPC], (5) vanadyl-tetrasulfophthalocyanine [VOTSPC], (6) cobalt(II) tetraaminophthalocyanine [Co(II) TAPC], and (7) chloroiron(III) tetraaminophthalocyanine [ClFe(III) TAPC].

We tested the synthesized phthalocyanines for corrosion inhibition, first by the linear polarization resistance method on mild steel in a typical naval environment (1% NaCl at pH = 2) and then with slow potentiodynamic experiments and AC-impedance analysis to obtain information on the inhibition of anodic and cathodic reactions of steel in the naval environment. The seven water-soluble phthalocyanines were not very effective corrosion inhibitors. Apparently, these highly water soluble complexes are not adsorbing effectively to the metal surfaces. We used two approaches to improve the adsorption effectiveness: polymeric coatings of the phthalocyanine were prepared on the metal surfaces, and derivatives of the phthalocyanines that contain long alkyl chains to increase adsorption were also synthesized.

We synthesized polymeric coatings of phthalocyanines by decarboxylation of chloroiron(III) tetracarboxyphthalocyanine [ClFe(III) TCPC]. The coatings were found to inhibit corrosion of mild steel up to 82%. The polymers are sheet polymers having a graphitic type structure, with voids between the phthalocyanine units. We formed phthalocyanine derivatizes with long alkyl chains by converting the tetracarboxyphthalocyanines to the corresponding acid chloride and reacting the acid chloride with amino acids containing 6 or 12 carbons in the alkyl chain

that connects the amine and acid functionalities. Four compounds were synthesized containing Co(II) or Fe(III) and either C_6 or C_{12} alkyl chains. These phthalocyanine derivatives were applied to steel by dip-coating and then tested for corrosion inhibition. These materials show inhibition efficiencies of up to 88%.

We surveyed the effect of the central metal ion on the corrosion efficiency of each polymeric phthalocyanine and the long alkyl chain derivatized phthalocyanines. We tested Zn(II), OV(IV), Cr(III), and Si(IV) as the central metal ion. The long alkyl chain Zn(II) material [Zn(II) TCAUPC] showed significantly improved corrosion inhibition efficiencies.

One of the problems with all these systems is that the inhibition is limited to steel; we do not see similar efficiencies for aluminum. To improve the inhibition effectiveness, we first treated the aluminum with an aminosilane then reacted it with the tetraacidchloride-phthalocyanine to improve the binding of the phthalocyanine to the aluminum surface. Our preliminary results showed that this technique was effective on aluminum.

We also attempted to increase the efficiency of the polymeric phthalocyanine coatings by filling the voids in the sheet polymer. We have attempted several strategies for filling the void, all involving synthesis of new phthalocyanines that have reactive groups at the positions on the phthalocyanine that are in the void after polymerization. To date, these approaches have not improved corrosion inhibition.

In summary, we have demonstrated that macrocyclic corrosion inhibitors of the phthalocyanine type show promise in a number of forms. The high thermal and mechanical stability of these materials and their low cost make them attractive candidates for practical corrosion-inhibiting coatings.

CONTENTS

FIGURES

TABLES

INTRODUCTION

SRI conducted this project for the Naval Air Development Center under Contract No. N62269-85-C-0290 to synthesize macrocylic compounds and perform laboratory experiments to evaluate their performance as multipurpose corrosion inhibitors for metals in a naval environment.

Attempts have been made in the past to synthesize and test the effectiveness of macrocyclic compounds, such as porphyrins, as corrosion inhibitors for pure iron in media containing chloride. Macrocycles of these types are extremely stable compounds that would form stable corrosion inhibitors. Porphyrins have been found to interact strongly with metallic surfaces by coordination[1] and by π-orbital interaction with the electrons in the d-orbitals of the metal.[2]

A variety of porphyrins having different degrees of polarity have been synthesized and tested recently for their corrosion inhibition properties.[3] Previous studies on these compounds have been confined mainly to porphyrins with aromatic substituents at the meso positions. Investigations have shown that these porphyrins are reasonably effective as corrosion inhibitors for iron in chloride media.

Data on the use of phthalocyanines as corrosion inhibitors are scarce. The information available in the literature is confined to the use of lead and sodium phthalocyanines as corrosion inhibitors for steel[4] and aluminum,[5] respectively.

The mechanism of corrosion inhibition with macrocyclic systems is mostly due to the chemisorption of the organometallic macrocycle onto the metal surface. One factor that enhances the degree of chemisorption is the planarity of the molecule. A planar molecule is expected to increase the interaction between the π-electron system of the macrocycle and the conduction band of the metal. Furthermore, the planar molecules are expected to provide a high degree of coverage and hence a higher inhibitor efficiency.

Snow and Jarvis[6] showed that the planarity and electron density in the π-electron-system of macrocycles affect their surface adsorption properties and that the phthalocyanine compounds are particularly useful for the formation of stable films. For this reason, we synthesized phthalocyanines having the generalized structure shown in Figure 1, which are considered to be almost rigidly planar.[7-12]

Longo[3] reported that higher water solubility of compounds might increase their inhibitor efficiency. To test this hypothesis, we

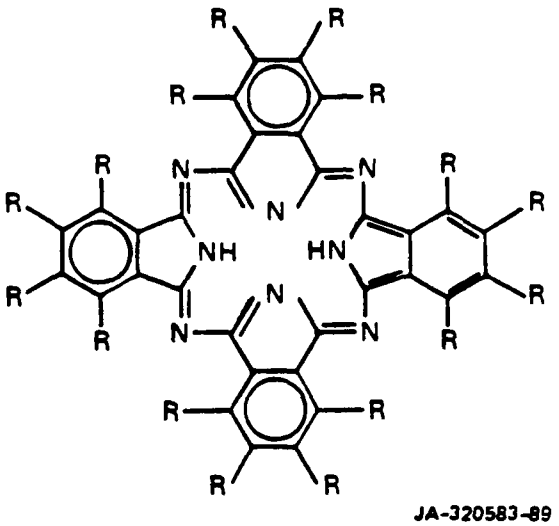

Figure 1. General structure of phthalocyanine.

synthesized highly water soluble tetrasulfophthalocyanines with a variety of metal ion centers. In fact, the first few phthalocyanines we synthesized satisfied both the planarity and water solubility requirements.

We also synthesized and tested the water-insoluble tetraamino-phthalocyanines, tetracarboxyphthalocyanines, and phthalocyanines having C_5 and C_{10} aliphatic hydrocarbon chains attached to them. The application of water-insoluble phthalocyanines to the surface by dip coating was followed by a suitable heat treatment.

Because we did not have much success with water-soluble phthalocyanines, we concentrated on forming stable polymeric phthalocyanine films on the metal surface. Steel with a poly Fe(III) TCPC coating had inhibition efficiencies of about 82%. We believe that this finding is significant because the polymeric coating, in addition to inhibiting corrosion is also a good electronic conductor when doped. This property extends the use of these polymeric films in applications involving EMI coatings.

Water-insoluble phthalocyanines having long-chain alphatic carboxylic acid groups attached to them also provided significant corrosion inhibition of steel, as high as 88%. We tested four samples containing Co(II) or Fe(III) as the central metal ion and either a C_6 or C_{12} carboxylic acid group. The highest corrosion inhibition efficiencies were found with the longer carboxylic acid derivatives. The long alkyl chains interact with each other because of Van der Waals forces, forming a protective hydrophobic layer on the metal surface. We believe that the high corrosion inhibition efficiency exhibited by long alkyl chain containing phthalocyananines is a signficant finding because these coatings only require a low temperature heat treatment at 110°C.

We surveyed the effect of central metal ion on both the polymeric phthalocyanines and the long-chain derivatized phthalocyanines. In addition to the cobalt(II) and iron(III), we tested zinc(II), chromium(III), vanadium(IV), and silicon(IV). Among the metal ions tested, zinc shows the most promise of significantly improving the corrosion inhibition efficiency.

The polyphthalocyanines formed when the tetracarboxyphthalocyanines are heat treated contain structual voids between phthalocyanine monomer units, as shown in Figure 2. We believe that the corrosion inhibition efficiency of the polyphthalocyanine coatings can be further improved if these voids are filled with organic molecules that show corrosion inhibition on their own and provide additional anchoring points onto the metal surface. Thus, during this period of research, we have designed a derivative of phthalocyanine in which the voids are filled with pyridine groups, as shown in Figure 3. Our approach involves the synthesis of nitro-substituted tetracarboxyphthalocyanine that is the precursor of polyphthalocyanine. The substituent group will be replaced by a pyridine group and then polymerized on the metal surface by a heat treatment.

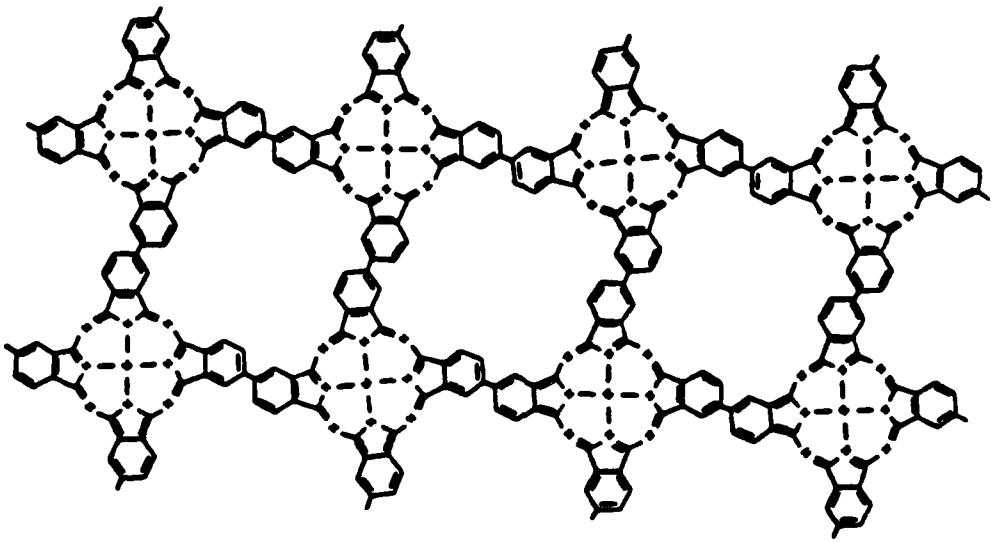

RA-1178-6

Figure 2. The structure of the polymer formed during the heat treatment of tetracarboxyphthalocyanine.

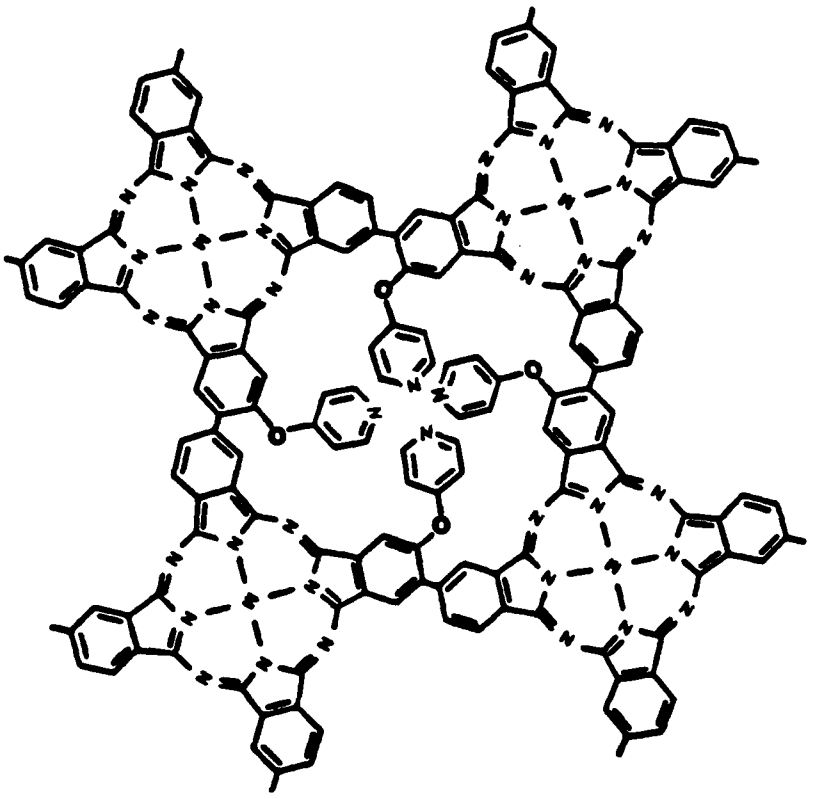

RA-1178-27

Figure 3. The structure of void-filled polymeric phthalocyanine.

Because of the poor π-electron accepting ability of aluminum, phthalocyanine coatings do not adhere to aluminum surfaces well and therefore do not provide the inhibiting action they provide on steels. Thus, the interaction of the phthalocyanine molecules with an aluminum surface is weaker than its interaction with a steel surface. However, because silanes adsorb well on aluminum-7075 alloy (see our last annual report), we synthesized a phthalocyanine derivative that contains a silane substituent. Our approach was to coat the aluminum surface with a silane compound and then react the silane with a phthalocyanine derivative. The results of these studies are described in detail in the following sections.

EXPERIMENTAL DETAILS

Synthesis

General Methods

Materials. We obtained the necessary materials from various sources. We purchased thionyl chloride, 6-amino-caproic acid, 11-aminoundecanoic acid, sodium hydroxide, trimethylbenzene, pyridine, 1,2,4-trimellitic anhydride, aminopropyl-triethoxysilane, urea, sodium dithionite, and 1,2,4-benzenetricarboxylic anhydride from Aldrich. We prepared the monosodium salt of 4-sulfophthalic acid by adding 1 equivalent of sodium hydroxide to a 50% aqueous solution of 4-sulfophthalic acid (Kodak) and then drying under vacuum for 5 days. We purchased potassium cyanide, ammonium molybdate, ferrous sulfate, and zinc chloride from Mallinkrodt; vanadyl chloride from Alfa; silicon tetrachloride from Petrach; and sodium sulfide, chromium trichloride, bromine, chloroform, acetic anhydride, sulfuric acid, and nitric acid from J. T. Baker Chemical Co. All chemicals were used without further purification.

Physical Measurements. We measured the UV-visible spectra and kinetic studies with a Hewlett-Packard 8450A spectrophotometer and recorded NMR spectra on a JOEL FX90Q spectrometer. Microanalyses were performed by Galbraith Laboratory or measured by a Perkin-Elmer 240-XA elemental analyzer. We determined magnetic susceptibilities by the Evans method.[13] In a typical run, a solution of $\sim 10^{-2}$ M D_2O of the metal complex containing 1% of tert-butyl alcohol as an internal reference was placed in a 5 mm NMR tube equipped with a 2 mm coaxial inner tube. A 5% tert-butyl alcohol in D_2O without the metal complex was placed in the inner tube, which served as an external reference. The difference between the chemical shifts of the two references is measured by ^1H NMR. The magnetic susceptibility χ of the metal complex is calculated according to the following equation:

$$\chi = \frac{3\Delta f}{2\pi f m} + \chi_o + \frac{\chi_o (d_o - d_s)}{m} \qquad (1)$$

where Δf is the frequency separation between the two lines, f is the frequency at which the proton resonances are being studied, m is the mass of the metal complex contained in 1 mL of solution, χ_o is the magnetic susceptibility of the solvent, d_o is the density of the solvent, and d_s is the density of the solution. The last term is neglected in our calculation. Magnetic moments, μ_{eff}, can be calculated by the following equation:[14]

$$\mu_{eff} = 2.84 \sqrt{\chi_m T} \qquad (2)$$

Correction factors due to the solvent and the metal-free phthalocyanine, -0.72×10^{-6} and -550×10^{-6}, respectively, are applied.

Purity of the Compounds Synthesized. The phthalocyanine complexes prepared contain various amounts of water molecules. Elemental analyses do not provide adequate assurance of purity because of the high formula weights and other difficulties.[14] Magnetic susceptibility measurements are suggested as an alternative method. Table 1 lists the magnetic moments of the five complexes prepared in this work. They are in reasonable agreement with those reported by Busch and Weber,[15,16] although different methods were used. The magnetic moment for Fe(II) TSPC has not been reported. In general, a value of 3.3 B.M. for Fe(II) complexes indicates that the metal is at an intermediate spin state of S = 1 and S = 2, which is usually observed in the iron(II) porphyrin compounds.[17,18]

UV-visible spectra also provide valuable information on the purity of the complexes. In the preparation of Co(III) TSPC, we noted that incomplete oxidation of Co(II) TSPC may be the major source of impurities. The UV-visible spectrum of Co(II) TSPC has an intense absorption at 658 nm, which shifts to 672 nm on oxidation to Co(III) TSPC. Similarly, Fe(II) TSPC may be contaminated by Fe(III) TSPC because of the insufficient reduction or air oxidation. Absorptions at 634 nm due to the Fe(III) TSPC and at 670 nm due to the Fe(II) TSPC can be used as an indication of purity. The UV-visible spectral data for the metal phthalocyanine complexes are listed in Table 2.

Synthesis of Water-Soluble Phthalocyanines

Tetrasodium Salt of Cobalt-4,4',4',4'"-Tetrasulfophthalocyanine 3-Hydrate, Co(II) TSPC·$3H_2O$. The preparation procedure is adapted from that reported by Busch and Weber.[15] A mixture of monosodium salt of 4-sulfophthalic acid (57.8 g., 1.2 mol), ammonium chloride (10.3 g, 0.2 mol). ammonium molybdate (1.2 g, 0.001 mol), cobalt(II) sulfate 7-hydrate (28 g, 0.06 mol), and nitrobenzene (60 mL) is added to a 500 mL, three-necked flask fitted with a reflux condenser and a mechanical stirrer. The mixture is heated slowly to 150°C for 0.5 h with continuous stirring or until the gas evolution ceases. The temperature is raised to 180°-190°C and maintained for 5 h. Nitrobenzene (200 mL) is slowly added while the mixture is still hot.

The solid product is filtered, washed with 500 mL of methanol, ground to powder, and washed again with 500 mL of methanol. The remaining solid is added to 1 L of 1 N HCl saturated with NaCl. The solution

Table 1

MAGNETIC MOMENTS OF THE PHTHALOCYANINE COMPLEXES

Compound	Magnetic Moment μ_{eff} (B.M.)	
	This work*	Reported§
Co(II) TSPC	1.95 ± 0.08	1.88 ± 0.05
Co(III) TSPC	0.73 ± 0.09	0.74 ± 0.05
Fe(II) TSPC	3.30 ± 0.05	--
Fe(III) TSPC	2.08 ± 0.01	1.80 ± 0.05
VOTSPC	Diamagnetic	

*Measured by ^1H NMR operated at 89.55 MHz in $\sim 10^{-2}$ M D_2O solution at 27° C.

§From References 15 and 16.

Table 2

UV-VISIBLE ABSORPTION DATA
OF THE METAL PHTHALOCYANINE COMPLEXES*

Complex	λ_{max} (n,m), (10^{-4} ε)
Co(II) TSPC 214	(7.13)
320	(7.32)
630	(6.19)
658	(6.3)
Co(III) TSPC 214	(6.50)
284	(5.04)
326	(5.36)
672	(8.25)
Fe(II) TSPC 221	(8.44)
322	(8.74)
430	(1.95)
610	(3.45)
670	(11.50)
Fe(III) TSPC 218	(7.24)
285	(4.10)
328	(5.87)
634	(7.12)
VOTSPC 218	(9.70)
346	(9.07)
658	(12.11)
688	(8.92)

*Concentrations are about 1 x 10^{-5} M.
The optical cell pathlength is 1 cm.

and accompanying undissolved material are heated to boiling for 5 min, cooled, and filtered. The HCl treatment is repeated once.

The solid collected from filtration is dissolved in 1 L of hot (~80°C) 0.1 N NaOH solution. Insoluble impurities are immediately separated by filtration. Sodium chloride (300 g) is added slowly to the solution, and the solution is then heated to 80°C for 3 h. The product is obtained by filtering the hot solution. This reprecipitation process is repeated two additional times. The solid collected is washed with 500 mL of 80% aqueous ethanol and then boiled for 4 h in 400 mL of absolute ethanol. The blue product is filtered and dried under vacuum at 150°C for 24 h (yield = 36.3 g, 70%).

Anal. Calcd for $C_{32}H_{18}N_8O_{15}S_4Na_4Co$: C, 37.04; H, 1.75; N, 10.80. Found: C, 37.07; H, 1.77; N, 10.77.

Tetrasodium Salt of Cobalt(III)-4,4',4'',4'''-Tetrasulfophthalocyanine 3 Hydrate, Co(III) TSPC·$3H_2O$. The Co(II) TSPC is oxidized by air in the presence of 3 equivalents of cyanide ion to Co(III) TSPC.[16] To 250 mL of 0.5 M Co(II) TSPC (6.12 g, 6.25 mmol) at a pH of 8 is added 10 mL of 0.125 M sodium cyanide solution (0.163 g, 12.5 mmol). Air is bubbled through the solution for 4 days. Solvent is evaporated under reduced pressure. Ethanol (100 mL) is added, and the mixture is heated to boiling. The solid is collected by filtration and is extracted for 3 h in a Soxhlet extractor with 300 mL of absolute ethanol. The dark green solid is collected and dried at 150°C under vacuum for 24 h (yield = 6 g, 96%).

Anal. Calcd for $C_{32}H_{19}N_8O_{16}S_4Na_4Co$:C, 34.76; H, 1.73; N, 10.13. Found: C, 34.79; H, 1.81; N, 10.62.

Tetrasodium Salt of Hydroxy Iron(III) 4,4',4'',4'''-Tetrasulfophthalocyanine 3 Hydrate, Fe(III) TSPC·$3H_2O$. The preparation procedure is similar to that for Co(II) TSPC described above with the substitution of ferrous sulfate for cobalt sulfate. The yield was 40%.

Anal. Calcd for $C_{32}H_{19}N_8O_{16}S_4Na_4Fe$: C, 36.69; H, 1.83; N, 10.69. Found: C, 36.02: H, 1.84; N, 10.58.

Tetrasodium Salt of Iron(III) 4,4',4'',4'''-Tetrasulfophthalocyanine 3-Hydrate, Fe(II) TSPC·$3H_2O$ This compound is obtained by the reduction of the Fe(III) TSPC with sodium dithionite. All manipulation is done in a nitrogen-filled glove box. Fe(III) TSPC (3.47 g, 3mmol) is dissolved in 100 mL of H_2O (degassed by bubbled nitrogen for 1 h). An aqueous solution of sodium dithionite (0.3 M) is added dropwise to the Fe(III) TSPC solution until the UV-visible spectrum shows that the 632-nm peak has disappeared, which is attributed to the Fe(III) species. Sodium chloride (100 g) is added and the solution is allowed to stir for 3 h. The powder product is filtered, washed with 30 mL of 95% ethanol, and recrystallized from water and ethanol. The pure product is collected and dried at 150°C under vacuum for 24 h (yield = 2.5 g, 73%).

Anal. Calcd for $C_{32}H_{18}N_8O_{15}S_4Na_4Fe$: C, 37.23; H, 1.85; N, 11.13.

Found: C, 37.43; H, 1.81; N, 1.18.

Tetrasodium Salt of Oxovanadium(IV) 4,4',4'',4'''-Tetrasulfophthalocyanine·8 Hydrate·2 NaCl, VOTSPC $8H_2O$ 2NaCl. The vanadium derivative is obtained using the procedure of Farina et al.,[18] which is a modification of the Weber and Busch procedure. A mixture of the monosodium salt of 4-sulfophthalic acid (17.36 g, 0.068 mol), urea (23.32 g, 0.3880 mol), ammonium chloride (1.92 g, 0.0360 mol), ammonium molybdate (2.96 g, 0.0002 mol), and vanadylsulfate (4.20 g, 0.0192 mol) is ground to a fine powder. The powdered mixture is added slowly over a 15 min period to 16 mL of nitrobenzene, which is held between 170°C and 190°C in a three-necked flask equipped with a reflux condenser and a mechanical stirrer. Strong gas evolution is observed. After 30 min, 15 mL additional nitrobenzene is added. After 1 h, the temperature is increased to 200°C and held for 5 h.

The cooled flask contains a black solid covered by a brownish liquid. The solid is washed with 95% ethanol. The collected solid is pulverized in a mortar and slurried in 150 mL of 95% ethanol overnight. The solid is filtered and then slurried in 200 mL H_2O with 6 mL of concentrated H_2SO_4 that has been saturated with Na_2SO_4. The mixture is refluxed for 5 min, cooled, and filtered. The solid is dissolved in 300 mL of 0.1 N NaOH, heated to 90°C, and filtered warm. The filtrate is diluted with 200 mL of saturated NaCl solution and heated to 90°C for 15 min. The solution is cooled in an ice bath, and slowly a fine dark-blue precipitate forms. The dark-blue solid is collected by filtration and washed with 300 mL 80% ethanol. The solid is refluxed with 100 mL of 100% ethanol for 4 h, filtered hot, washed with 3 x 20 mL portions of 100% ethanol, and dried in a vacuum dessicator for 48 h (yield = 6.3 g, 42%).

Anal. Cald for $C_{32}H_{19}N_8O_{16}S_4Na_4Co$: C, 30.75; H, 2.24; N, 8.97; V, 4.08; Na, 11.05; Cl, 5.69, H_2O, 11.53; S, 10.25. Found: C, 28.58; N, 9.02; V, 3.38; Na, 11.3; Cl, 4.05; H_2O, 10.50; S, 10.69.

Co(II) 4,4',4'',4'''-Tetranitrophthalocyanine. Cobalt (II) chloride hexahydrate (9 g, 0.038 mol), 4-nitrophthalic acid (25.76 g, 0.122 mol), urea (31 g, 0.517 mol), and ammonium molybdate (0.2 g, 0.0002 mol) were finely ground and placed in a 500-mL three-necked flask equipped with a mechanical stirrer and reflux condenser. Nitrobenzene (130 mL) was added, and the mixture was heated in an oil bath at 130°C for 0.5 h with continous stirring. After gas evolution ceased, the mixture was heated to 190°C for 5 h and filtered hot. The solid was washed with 500 ml of methanol and dried. The crude product was added to 900 mL of 1 N HCl, boiled for 1 h, cooled to room temperature, filtered, and washed with 200 mL H_2O. The purple powder was washed with 800 mL H_2O. The purple powder was next treated with 800 mL 1 N NaOH and heated to 90°C for 2 h. The product was filtered and washed with 200 mL H_2O. The HCl and NaOH treatments were repeated twice. The product was finally washed with 200 mL methanol and dried under vacuum for 16 h (yield = 18.3 g, 80%).

Co(II) 4,4',4'',4'''-Tetraaminophthalocyanine Tetrahydrochloride. Co(II) 4,4,'4'',4'''-tetranitrophthalocyanine (5 g) was finely ground and placed in a 250 mL round-bottomed flask. Excess sodium sulfide nonahydrate was added and stirred at 50°C for 5 h. The mixture was allowed to cool and stand overnight. The clear solution was decanted, and the slurry was filtered and washed with 50 mL of H_2O. The solid was added to 500 mL of 1 N HCl and heated to a boil for 0.5 h. The solution was cooled to room temperature and filtered. The solid was added to 500 mL of NaOH, boiled for 2 h, filtered, washed first with 50 mL of H_2O, and then 200 mL of methanol. The solid was added to 500 mL of 1 N HCl, boiled for 0.5 h, and cooled to room temperature. The product was collected by filtration, washed with 50 mL H_2O and 200 mL methanol, and dried at 150°C under vacuum for 3 h (yield = 4.5 g, 86%).

Anal. Calcd for $C_{32}H_{34}N_{12}Cl_4Co$: C, 49.44; H, 3.11; N, 21.62. Found: C; 49.75, H, 2.38; N, 22.29.

Chloro-Fe(III) 4,4',4'',4'''-Tetraaminophthalocyanine Tetrahydrochloride. This compound was prepared by the same method as that described above, using ferrous sulfate heptahydrate in place of cobalt chloride (yield = ~30%).

Anal. Calcd $C_{32}H_{24}N_{12}Cl_5Fe$: C, 47.47; H, 2.99; N, 20.76. Found: C, 49.57; H, 3.04; N, 20.31.

Synthesis of Polymeric Phthalocyanines

Tetracarboxyphthalocyanines were prepared by methods very similar to that reported by Shirai et al.[19] The tetracarboxyphthalocyanine was converted to the polymer on the the metal surface according to the method of Achar et al.[20]

Co(II) or Fe(III) Tetraamidophthalocyanine. The solid reagents 1,2,4-benzenetricarboxylic anhydride (0.1 mol), urea (0.6 mol), ammonium chloride (0.02 mol), ammonium molybdate (10.0005 mol), and the corresponding metal chloride (0.03 mol) were finely ground in a mortar. The powder reagents and 300 mL of nitrobenzene were loaded into a 500 mL, three-necked, round-bottom flask. A mechanical stirrer was fitted to the middle neck. The two side necks were each fitted with a reflux condenser. One condenser was connected to a nitrogen inlet and the other to a bubbler. The mixture was heated in an oil bath at 160°C for 5 h. A low stream of nitrogen was constantly swept through the system during the heating period. After cooling, the greenish-black solid was crushed and washed with 500 mL of methanol, 200 mL water, and then 30 mL of methanol again. The product was dried under vacuum for 24 h.

Co(II) or Fe(III) Tetracarboxyphthalocyanine. The tetraamidophthalocyanines (5 g) were hydrolyzed by boiling in 1 L of 1 NaOH for 6 h. Sodium chloride (~200 g) was added to the hot solution and the mixture was allowed to cool to room temperature. The blue powder was collected by filtration, added to 500 mL of 1 N HCl, heated to boiling, and fil-

tered. The product was washed with 300 mL of 95% ethanol and dried under vacuum overnight. The sodium salts of these compounds were obtained by repeating the NaOH treatment.

Anal. Calcd for $C_{36}H_{18}N_8O_{11}Na_4$ Co: C, 48.61; H, 2.04; N, 12.60. Found: C, 48.33; H, 2.27; N, 12.88.

Polymerization of Co(II) or Fe(III)-Tetracarboxyphthalocyanine on Steel and Aluminum Surfaces. We investigated the possibility of forming stable phthalocyanine polymer coatings on the metal surface instead of using a simple dip-coating procedure with the monomer. A polymer coating is expected to remain more stable under varying hydrodynamic conditions, thereby bringing about high corrosion inhibition rates even under the influence of the shearing forces operating on the polymer-coated surface.

The coating solution was prepared by dissolving 100 mg of Co(II)-tetracarboxyphthalocyanine [Co(II) TCPC] in 5 mL of dimethyl sulfoxide (DMSO) and immersing the polished (400 grit) and degreased (in ethanol) metal sample in this solution for 12 h.

The metal sample was then removed from the coating solution and introduced into a furnace sparged with argon gas. The sample was then heat treated at 450°C for 1.25 h in the inert atmosphere, during which process an adherent and stable phthalocyanine polymer coating was formed.

The in-situ polymerization of tetracarboxyphthalocyanine was first observed by Achar et al.[20] The polymerization reaction occurs with the loss of H_2O, CO, and CO_2, as detected by gas chromatography and IR spectroscopy. The reaction apparently is multistep; loss of water gives the anhydride as an intermediate, shown in reaction 1. The anhydride thermally decomposes through the loss of CO and CO_2 to give the polymeric product (Figure 2) in which the phthalocyanines are linked by a covalent bond between benzene rings.

We adapted the method of Achar et al.[20] to polymerize monomeric tetracarboxyphthalocyanines adsorbed on a metal electrode surface. To prepare Fe(III) TCPC polymer coatings, we increased the concentration of the phthalocyanine solution by dissolving 150 mg of Fe(III) TCPC in 5 mL of DMSO instead of using 100 mg of the compound in the same volume of DMSO. We increased the concentration to minimize the porosity of the polymer coating. Some experiments were performed with multiple coatings as well as with samples preetched in 1% NaCl solution (pH = 2) before the phthalocyanine treatment.

Zn(II), OV(IV), Cr(III), and Si(IV) Tetracarboxyphthalocyanines. The silicon-, zinc-, chromium-, and vanadyl-centered TCPCs were prepared in the same manner as the Co(II) TCPC and Fe(III) TCPC discussed above.

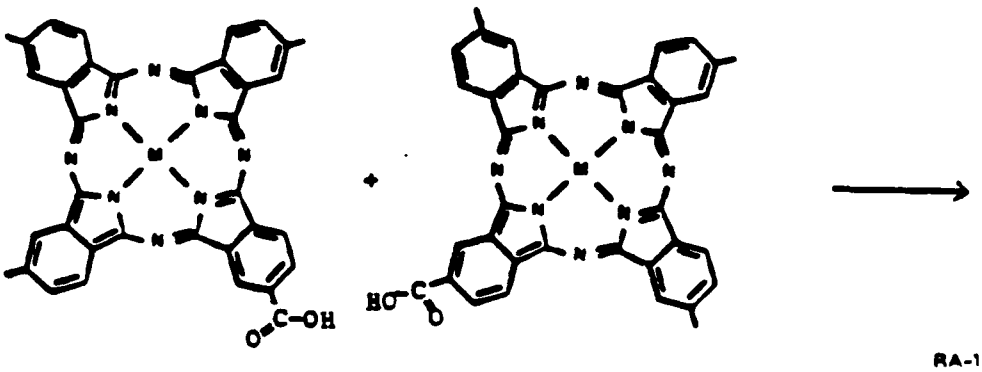

RA-1178-28

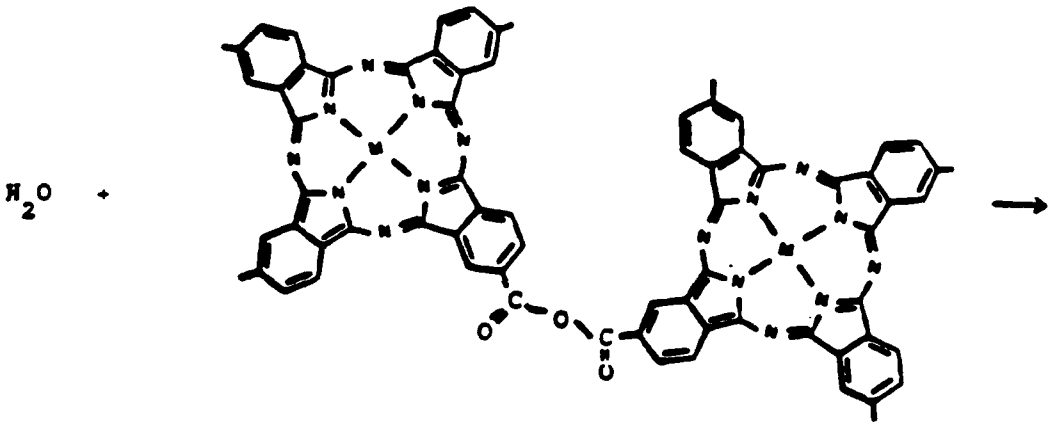

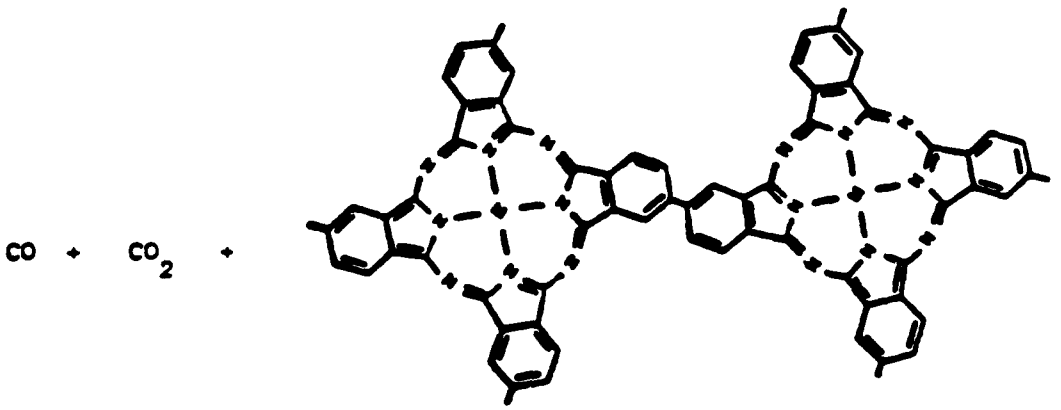

[1]

Synthesis of Long-Chain Carboxylic Acid Substituted Phthalocyanines

The tetraacidchloride derivatives were prepared from the corresponding tetracarboxyphthalocyanine by methods similar to those reported by Shirai et al.[19]

Co(II) or Fe(III) Tetracarbonylchlorophthalocyanine. Into a 50 mL round-bottom flask, 5 g of the finely ground metal tetracarboxyphthalocyanine, 15 mL of thionyl chloride, and a few drops of pyridine were added. The mixture was allowed to reflux overnight under a nitrogen atmosphere. Excess thionyl chloride was removed by vacuum. The product was washed with 3 x 20 mL dry toluene and then dried under vacuum for 2 days.

Co(II) or Fe(III)-Tetrakis (N-Carboxyl-6-amino-caproic acid)-phthalocyanine[TCACPC]. A solution of 6-amino-caproic acid (10.98 g, 4.88 mmol) and 4.88 mL of 1 N NaOH was added to a 100 mL, three-necked, round-bottom flask that was equipped with a powder addition funnel and a liquid addition funnel. Tetracarbonylchlorophthalocyanine (1.22 mmol) was added to the powder addition funnel, and 4.88 mL of 1 N NaOH was added to the liquid addition funnel. The amino acid solution was cooled in an ice bath with rapid stirring. The tetracarbonylchlorophthalocyanine and NaOH were added simultaneously to the solution in 10 portions during a 1 h period. The resulting solution was stirred for another 0.5 h and then acidified to a pH of 3 with 1 N HCl. The product precipitated in very fine powder form and was collected by centrifuging. The greenish-black powder was washed twice with 20 mL of slightly acidified water and then with 20 mL of petroleum ether. The product was placed in a vacuum dessicator and dried under vacuum overnight.

Co(II) or Fe(III)-Tetrakis (N-Carboxyl-12-Aminoundecanoic Acid)-phthalocyanine[TCAUPC]. The syntheses of these compounds were similar to that of the caproic acid analog, but the corresponding amino acid was dissolved in 24.4 mL of 0.2 N NaOH because of its low solubility.

Zn(II), OV(IV), Cr(III), and Si(IV) Tetracarbonylchlorophthalocyanines. All glassware was dried in an oven and cooled under N_2. Two grams (2.4×10^{-3} mol) of the metal tetracarboxyphthalocyanine, 6 mL (8.29×10^{-2} mol) of thionyl chloride, a few drops of pyridine, and a stir bar were added to a 25 mL three-necked, round-bottom flask fitted with a condenser and nitrogen inlets. The mixture was allowed to reflux overnight under a nitrogen atmosphere. Excess thionyl chloride was removed by vacuum.

Zn(II), OV(IV), Cr(III), and Si(IV) Tetrakis (N-Carbonyl-II-Aminoundecanoic acid) Phthalocyanine. A solution of 11-aminoundecanoic acid (2.00 g, 10.16 mmol) and 1 N NaOH (5 mL) was added to a 100 mL three-necked, round-bottom flask equipped with a powder addition funnel and a liquid addition funnel. Tetracarbonylchlorophthalocyanine

(2.0 g, 2.5 mmol) was added to the powder addition funnel, and 5 mL of 1 N NaOH solution was added to the liquid addition funnel. Equal amounts of material from each funnel were added over 1 h under a steady static flow of nitrogen. The resulting solution was stirred overnight. Excess water was pulled off by vacuum. The collected powder was dried overnight in a vacuum desiccator.

The general structure of these phthalocyanines containing long alkyl chains is shown in Figure 4.

Phthalocyanine Coatings on Aluminum

Aluminum plates (1.5 x 1 x 1/8 inch) were cleaned with ethanol in an ultrasonic bath for 1 h, dried, then dipped in aminopropyltriethoxysilane for 1 min. The plates were quickly dipped in ethanol and then soaked in a DMSO solution of Fe(III) tetracarbonylchlorophthalocyanine (TCPC) overnight. The plates were dried under argon at 100°C.

Synthesis of Low-Void-Fraction Phthalocyanine Coatings

We took two approaches to synthesizing this material: the first was to attempt to fill the voids after the polymer was synthesized, and the second was to attempt to fill the voids prior to polymerization.

Void-Filled Postpolymerization. This preparation involved four individual steps. First, we prepared the phthalocyanine precursor, 5-nitro-1,2,4-benzenetricarboxylic acid, by nitration of 1,2,4-benzenetricarboxylic anhydride. The tetranitrotetracarboxyphthalocyanine metal complex is obtained by the classical template synthesis. This compound is then polymerized on the metal surface. The nitro groups are finally substituted with para-oxypyridine groups to fill the void. The synthesis and the polymerization procedures are described above. The preparation of the phthalocyanine precursor and the substitution reaction are described below.

5-Nitro-1,2,4-Benzenetricarboxylic Acid. 1,2,4-Benzenetricarboxylic anhydride (100 g, 0.52 mol) is dissolved in 400 mL of concentrated H_2SO_4. Nitric acid (98%, 50 mL) is added, and the mixture is heated at 70°C for 16 h. The resulting yellow solution is poured on 300 g of ice and then cooled in an ice bath. The whole precipitate is collected by filtration and washed with ether. The product is recrystallized from hot water.

Iron (III) Tetranitro-Tetracarboxyphthalocyanine. The nitro-1,2,4-trimellitic acid (0.1 mol), urea (0.6 mol), ammonium chloride (0.02 mol), ammonium molybdate (0.0005 mol), and ferrous chloride (0.03 mol) were finely ground in a mortar. The powdered reagent and 300 mL of nitrobenzene were loaded into a 500 mL three-necked flask equipped with a mechanical stirrer, a condenser, and a nitrogen inlet. The mixture was heated to 160°C for 5 h, filtered, and washed with methanol and water. The green solid was collected and boiled in 1 L in NaOH for 6 h. Sodium chloride was added to the hot solution, and the mixture was allowed to

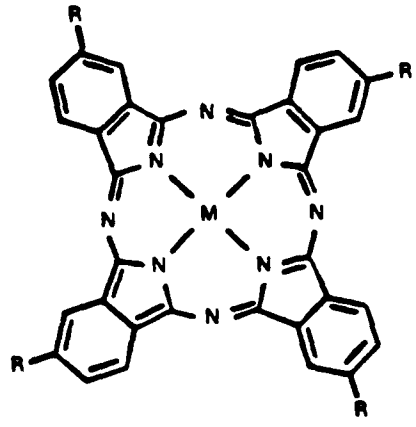

RA-m-1178-20

Figure 4. The general structure of phthalocyanine containing long-chain aliphatic (R) groups.
TCACPC: R = $CONH(CH_2)_5COOH$
TCAUPC: R = $CONH(CH_2)_{10}COOH$
M = Co(II) or Fe(III)

cool. The blue powder was collected by filtration, added to 500 mL of 1 N HCl, heated to boil, and filtered. The product was washed with 300 mL of 95% ethanol and dried under vacuum overnight.

Substitution of the Nitro Groups. The polytetranitrophthalocyanine-coated electrode is immersed in a solution of para-hydroxypyridine (1.0 g), potassium carbonate (1.0 g), and dried DMSO (10 mL) for 12 h. The electrode is then removed from the solution and rinsed with 0.1 N HCl, 0.1 N Na_2CO_3, and water.

Void Filled Prior to Polymerization

Our approach involved the synthesis of nitro-substituted tetracarboxyphthalocyanine, which is the precursor of polyphthalocyanine. The substituent groups were replaced by pyridine groups and then polymerized on the metal surface by a heat treatment.

3,5-Dinitro-1,2,4-Trimethylbenzene. 1,2,4-Trimethylbenzene (69.0 mL, 500 mmol) was suspended in H_2SO_4 (305 mL, 5.4 mmol); the resulting mixture was cooled on an ice bath; the HNO_3 (42.0 mL, 659 mmol) was added dropwise. The reaction was stirred at ice-bath temperature for 2 h and then poured into ice water (1000 mL). The solution was then extracted with CH_2Cl_2, the combined organic layers were washed with water and dried over sodium sulfate, and the solvents were removed by rotovapor. The resulting brown oil was flash-chromatographed on silica gel and eluted with CH_2Cl_2 to remove baseline contamination. The band collected from the column was then vacuum-distilled to provide 22.9 g (20%) of the 3,5-dinitro-1,2,4-trimethylbenzene as a yellow, crystalline solid: bp 118°-120°C (0.05 mmHg); mp 78°-81°C; ^1H NMR ($CDCl_3$) δ: 7.35 (s, ArH), 2.48 (d, 6H, CH_3), 2.30 (s, 3H, CH_3).

5-Bromo-1,2,4-Trimethylbenzene. 1,2,4-Trimethylbenzene (6.9 mL, 50 mol) was dissolved in chloroform (100 mL), and bromine (2.28, 44 mmol) was added. A small amount of Fe(s) filings were added, and the solution was heated at reflux for approximately 4 h. The solution was washed with water (150 mL x 2), dried over sodium sulfate, and rotovapped to a clear, colorless oil that partially crystallized on standing. The oil was put under vacuum overnight to remove any unreacted starting material, providing 6.7 g (67%) of the desired compound as a white, crystalline solid: mp 58°-61°C; ^1H NMR ($CDCl_3$) γ: 7.15 (d, 2H, ArH), 2.32 (s, 3H, CH_3), 2.20 (s, 6H, 2 x CH_3).

5-Nitro-4'-Oxypyridino-1,2,4-Trimethylbenzene. 3,5-Dinitro-1,2,4-trimethylbenzene (0.500 g, 2.38 mmol) and 4-hydroxypyridine (0.440 g, 4.63 mmol) were added to dry DMSO (30 ml) to give a yellow solution. Potasium carbonate (0.91 g, 6.59 mmol) was added, and the yellow suspension was stirred at 80°C. After 18 h, the brown suspension was cooled to 22°, filtered through glass wool into 50 ml H_2O, then acidified with HCl to give a brown solution with some tan precipitate. CH_2Cl_2 extraction (4 x 50 ml) of this mixture yielded an orange-brown solution that became yellow after washing with 2 x 50 ml 5% $NaHCO_3$. This solution was dried over $MgSO_4$ and reduced to an orange-brown, oily solid.

The solid was loaded with CH_2Cl_2 onto a 2-in. column of silica gel. CH_2Cl_2 then eluted a small amount of an unidentified orange-brown material. A major diffuse brown band was eluted with CH_2Cl_2:MeOH (10:1), which was collected and reduced to an orange-brown solid (200 mg, approx. 33%).

The ^1H NMR chemical shift and integration were consistent with the mono-substituted product 5-nitro-3-(4'-oxypyridino)-1,2,4-trimethylbenzene. ^1H NMR ($CDCl_3$/TMS, ppm): 7.27 (s, 1 H, Ar-H), 7.18 (d, J = 7.8 Hz, 2 H, pyr-H), 6.43 (d, J = 7.6 Hz, 2 H, pyr-H), 2.38, 2.34, 2.05 (3 singlets, 9 H, CH3).

5-Bromo-1,2,4-Tricarboxybenzene. 5-Bromo-1,2,4-trimethylbenzene (2.0 g, 10.04 mmol), $KMnO_4$ (11.42 g, 72.29 mmol), and Na_2CO_3 (1.40 g, 13.21 mmol) were added to 200 ml H_2O in a three-necked 500-ml flask fitted with a condenser to give a dark purple solution and white insoluble starting material. The mixture was heated to approximately 95°C with occasional scraping to return the subliming starting material back to the flask. After 3 days, ethanol was added until the reaction was no longer purple.

Hot filtering through celite gave a clear, colorless solution that was acidified with HCl and then stripped at 65°C on the rotovap to a hard, white solid. This solid was Soxlet extracted with acetone for 3 days and then the acetone solution was reduced to a pale beige solid (mp 210-214°C; lit. 203-208°C). Further purification by liquid-liquid extraction with ether/water for 36 h again gave a white solid (yield = 1.27 g, approx. 44%). ^1H NMR (D_2O, DSS): 8.12, 7.98 ppm. A minor peak of an impurity was present at 7.79 ppm. No Ar-CH_3 resonances were apparent.

Tetrabromophthalocyaninetetraamide (Br_4FeTAPC). 5 Bromo-1,2,4-trimethylbenzene (1.30 g, 4.50 mmol), NH_4Cl (0.048 g, 0.90 mmol), $(NH_4)_6Mo_7O_{24}$ (0.029 g, 0.0235 mmol), urea (1.62 g, 27.0 mmol), and $FeCl_2.4H_2O$ (0.268 g, 1.35 mmol) were powdered in a mortar pestle and added to a nitrogen-purged, three-necked flask fitted with a condenser and a mechanical stirrer. Twenty ml nitrobenzene were added. The suspension was stirred under nitrogen while heating to 160°C. (Urea sublimed into the condenser.) After 20 h, the dark brown-green product was cooled to room temperature and the pale yellow supernatant decanted off. The solid was scraped out of the flask and washed with MeOH, then H_2O, and finally MeOH again to give an olive-green powder after drying (yield = 510 mg, 43% based on the triacid).

Experimental Solution and Sample Preparation

We made all measurements on either a mild steel or aluminum-7075 rotating disk or rotating cylinder electrode. The speed of rotation was kept constant at 1800 rpm in the rotating disk studies and at 255 rpm in the rotating cylinder studies. The experimental environment consisted of a 1% NaCl aqueous solution at pH = 2. Some experiments were also

performed in the same solution at pH = 8. In these initial studies, the phthalocyanine concentatration was kept constant at 1 mM. The corrosion inhibition results were compared for each compound at the same concentration.

For water-soluble phthalocyanines, the compound is introduced into the 1% NaCl solution to make it 1 mM with respect to the phthalocyanine. When the phthalocyanine is water-insoluble, the polished specimen electrode is immersed in a 1 mM solution of the compound in DMSO for 13 h, washed with DMSO, dried at 100°C, and then introduced into the cell for electrochemical studies.

We etched the samples by immersing them in a 1% NaCl solution (pH = 2) for 10 min and then immersing the sample in 1 mM solution of either Co(II) or Fe(III) tetraaminophthalocyanine in DMSO for 15 h. Thereafter, the sample was removed from the solution and heat treated at 100°C for 2 h. Before the sample was dip coated, it was pre-etched to introduce adsorbed chloride ions onto the metal surface, which will then adsorb the nitrogen quaternized tetraaminophthalocyanines more strongly.

Methods for Evaluating Corrosion Inhibitors and Coatings

We first rapidly screened the inhibitors by using the linear polarization resistance method followed by a slow potentiodynamic scan. These measurements were followed by AC-impedance measurements to obtain more information on interfacial adsorption. The theoretical bases for the measurements are described below.

Linear Polarization Resistance Method

In this method the potential (E) of the metal in the given environment is scanned within a range of ± 10 mV around the corrosion potential (E_{corr}), and the current (I) is continuously recorded. The polarization resistance (R_p) is then defined as

$$R_p = \left(\frac{\partial E}{\partial I}\right)_{E=E_{corr}} \tag{3}$$

Once R_p is known, the corrosion rate of the metal can be evaluated by using the Stern-Geary relationship,[21]

$$I_{corr} = \frac{b_a b_c}{2.303(b_a + b_c)} \cdot \frac{1}{R_p} \tag{4}$$

where I_{corr} is the corrosion current and b_a and b_c are the anodic and cathodic Tafel slopes, respectively. In these studies, however, an exact evaluation of I_{corr} is not required because I_{corr} is inversely proportional to R_p, and b_a and b_c are assumed to be constants for a particular metal in a given environment. Thus,

$$I_{corr} = \frac{K}{R_p} \quad (5)$$

where

$$K = \frac{b_a b_c}{2.303(b_a + b_c)} \quad (6)$$

The advantage of this method is that the R_p measurements can be performed much faster (15 min) than with other techniques, which require several hours or even weeks in the case of the weight loss technique to complete one measurement.

One must carefully use Equation 5 for corrosion rate measurements, however, because the K value need not remain constant in the presence and in the absence of the inhibitor. It may even vary from one inhibitor to another because of the possibility of having different anodic and cathodic Tafel slopes. These slopes are likely to be different because b_a and b_c are system-dependent parameters.

Slow Potentiodynamic Scan Method

In this method the potential E at the metal/solution interface is scanned from a potential negative to the free corrosion potential to a value more positive than the corrosion potential at a relatively slow scan rate (0.1 mV/s), and the subsequent current is recorded. The resulting polarization curve [E/log(i) plot] enables the evaluation of cathodic and anodic Tafel slopes (b_c and b_a), the corrosion current density (I_{corr}), and the magnitudes of anodic and cathodic current densities at any potential E. In addition, the polarization behavior of the metal in the test environment also provides information on the adsorption and desorption behavior of the inhibitor on the metal surface.

AC-Impedance Method

In the AC-impedance technique, the electrode impedance is monitored as a function of the frequency with the help of a Solartron Model 1250 frequency response analyzer while the metal sample is held under potentiostatic control. The frequency response is analyzed down to frequencies of 10 mHz or less, depending on the system studied. In this analysis, the high-frequency intercept of the real axis impedance gives the solution resistance (R_s), whereas the low-frequency intercept gives a summation of both R_s and the polarization resistance (R_p). Once R_p is known, the corrosion rate of the metal can be evaluated by using Equation 4.

AC-impedance spectra also provide information on the impedance of the inhibitor layer, the development of active sites such as pores in the inhibitor layer as a function of time, the adsorption capacitance arising

from the presence of the inhibitor, and the presence or absence of diffusional processes and potential-dependent surface relaxation processes associated with coverages by the inhibiting species at lower frequencies and by the anodic intermediate species at higher frequencies.[22-24] Thus, high-frequency data provide information on the inhibitor-coating characteristics governed by the adsorption capacitance, whereas low-frequency data provide information on Faradaic process and surface relaxation processes associated with inhibitor adsorption.

Corrosion Inhibitor Efficiency Evaluation

Corrosion inhibitor efficiency (IE) is defined as

$$IE = \left(\frac{I^{o}_{corr} - I^{I}_{corr}}{I^{o}_{corr}}\right) \times 100 \qquad (7)$$

where I^{o}_{corr} and I^{I}_{corr} are the corrosion currents of the metal in the absence and in the presence of the inhibitor, respectively. From Equations 5 and 7, we obtain

$$IE = \left(\frac{R^{I}_{p} - R^{o}_{p}}{R^{I}_{p}}\right) \times 100 \qquad (8)$$

where R_p and R^{I}_{p} are the polarization resistances in the absence and in the presence of the inhibitor, respectively. The IE measurement using Equation 8 can be performed either with the polarization resistance technique or with the AC-impedance technique.

Corrosion Inhibition Studies

The phthalocyanine compounds synthesized were tested for their inhibitor efficiency by the linear polarization resistance technique. The PAR Model 273 Potentiostat/Galvanostat used could scan the potential of the working electrode at an extremely slow scan rate of 0.05 mV/s. This slow rate is important in reliably measuring the linear polarization resistance R_p. Higher scan rates generally result in a hysteresis in the current-potential variation, thereby introducing a considerable error to the R_p estimation. Variation of current with applied potential was recorded on a HP 7035B x-y recorder.

For R_p measurements, a scan rate of 0.05 mV/s was used, and the potentiodynamic polarization, from which polarization curves were constructed, was performed at a scan rate of 0.1 mV/s. For linear polarization resistance studies, the potential was scanned from 5 mV cathodic with respect to E_{corr} to 5 mV anodic with respect to the same potential. The potentiodynamic polarization was performed beginning from -700 mV (SCE) up to about -350 mV (SCE), which adequately covers the regions of interest in the polarization curves for inhibitor effectiveness studies.

We performed AC-impedance measurements at the free corrosion potential by holding the potential at this value using a PAR Model 173 Potentiostat. The AC impedance was measured over a wide frequency range (1 kHz to 10 mHz or less) using a Solartron Model 1250 Transfer Function Analyzer. The evaluation of the corrosion behavior of a polymer-coated metal, such as that used in this case, is made possible by the wideband AC-impedance measurements, which provide information on both the resistive and the capacitive behavior of the interface.

The rotating cylinder electrode arrangement provides better hydrodynamics and renders much faster mass-transfer rates for reasonably slow rotational speeds. Thus, all experiments with phthalocyanine polymer-coated electrodes were performed with a rotating cylinder electrode at a rotational speed of 255 rpm.

Weight Loss Studies

Weight loss studies were initiated in 1% NaCl (pH = 2) solution for uncoated as well as coated specimens of both steel and aluminum. Steel specimens were coated with Fe(III) TCPC polymer, whereas the aluminum-7075 specimens were first treated with the aminopropyltriethoxysilane for 1 min, dipped in ethanol, followed by the Fe(III) TCPC treatment in DMSO overnight. The aluminum specimens were dried at 100°C under argon and then immersed in 1% NaCl (pH = 2) solution for weight loss studies. After immersion in the solution, the samples were washed to remove any corrosion products formed, washed in methanol, air dried, and weighed to obtain the weight loss over the period of testing.

Coating Studies

We have designed a new heating apparatus for the thermopolymerization of phthalocyanine. A small hole is drilled in each of the metal plates. The metal plates are hung vertically on a lattice and placed in a glass cylinder so that argon flow and heat can be applied evenly on both sides of the plates. This approach is different from our previous one in which the metal plates were horizontally placed inside the glass cylinder. We achieved more even coating polymerization using this method. The Fe(III) TCPC and the Co(II) TCPC coatings on steel plates were prepared for weight loss experiments and for AC-impedance tests. For comparison, another set of steel plates was prepared by a similar method, except that the excess TCPC was washed away with methanol before heat treatment. This washing gives a thinner but more even coating.

Three methods can be used to coat the aluminum plates with silane-substituted phthalocyanine: We can coat the aluminum plate with the silane precursor and then attach the phthalocyanine to it, or do the reverse; or we can prepare the silane-substituted phthalocyaninese before coating on the aluminum plate. We chose the first and the third approaches because we believe that silane will better adhere to the

RESULTS AND DISCUSSION

Water-Soluble Phthalocyanines

Synthesis

Seven water-soluble phthalocyanines were synthesized using slight modifications of literature procedures. Those seven were the tetrasulfonated phthalocyanines of Co(II), Co(III), Fe(II), Fe(III), and OV(IV), as well as the tetraaminophthalocyanines of Co(II) and Fe(III). The tetraaminophthalocyanines were prepared by reduction of the tetranitrophthalocyanines.

Corrosion Inhibition Studies

Preliminary experiments with two of the phthalocyanines, VOTSPC and Co(III) TSPC, were performed in 1% NaCl solution at pH = 8 in the presence of air under stationary conditions. The data show that neither VOTSPC nor Co(III) TSPC is acceptable as a corrosion inhibitor for mild steel in 1% NaCl at pH = 8 under stationary conditions because of their low inhibitor efficiencies.

Measurements were also made on mild steel in a 1% NaCl solution of pH = 2 using a rotating disk electrode at a rotation speed of 1800 rpm (30 Hz). The study included VOTSPC, Co(III) TSPC, Fe(III) TSPC, Co(II) TAPC.4HCl, Fe(III) TAPC.4HCl, and thiourea as the reference compound.

All the phthalocyanine compounds investigated activated the cathodic reaction, contrary to the behavior observed with thiourea on the cathodic reaction. This cathodic activation process may promote higher anodic currents to maintain electro-neutrality, which results in the observed activation of the corrosion process in some cases. The system shows large cathodic Tafel slopes varying from -300 to -475 mV/decade. High Tafel slopes of this magnitude are generally associated with diffusional processes, which in this case could be the diffusion of oxygen onto the metal surface. These high Tafel slopes might disappear if the experiments were conducted in a deaerated system. However, we believe that the presence of oxygen in the system simulates the actual practical situation more closely than in its absence.

The Cl-Fe(III) TAPC·4HCl coating appears to marginally inhibit the cathodic reaction while activating the anodic reaction during the initial stages of the anodic polarization curve. However, this coating shows a better degree of corrosion inhibition than the Co(II) TAPC·4HCl coating on the steel surface.

A similar corrosion inhibition study with these two coatings, Co(II) TAPC·4HCl and Cl-Fe(III) TAPC·4HCl, formed on etched (in 1% NaCl, pH = 2) mild steel was performed to evaluate whether preadsorbed chloride ions could promote corrosion inhibition to a greater extent. The results show that etching is beneficial in the case of the Co(II) TAPC·4HCl coating,although it is not beneficial with the Cl-Fe(III)TAPC·4HCl coating.

Polymeric Phthalocyanines

Synthesis

The condensation polymerization of tetracarboxyphthalocyanines occur by loss of water to give the anhydride followed by decomposition of the anhydride through loss of CO and CO_2, which leads to an extremely stable sheet polymer. These sheet polymers have been prepared for six different phthalocyanines that vary in the central metal ion [Co(II), Fe(III), Zn(II), Cr(III), V(IV), and Si(IV)]. The polymerization reactions occur readily at 450°C.

Corrosion Studies

AC-Impedance Studies on Steel. Figure 5 compares the Nyquist plots [Re(Z) vs Imag(Z)] of the interfacial impedance as a function of frequency for the steel/solution interface without an inhibitor or a coating present on its surface as against a surface containing three polymer coatings of Co(II) TCPC and a single polymer coating of Fe(III) TCPC. The impedance spectra yield R_p values of 42.1, 133.6, and 238.6 Ω cm^2. The interfacial capacitance obtained from the R_p and the frequency at the maximum Imag(Z) are 378, 707, and 266 $\mu F/cm^2$. The relatively large capacitances are attributed to the presence of adsorbed chloride ions at the metal/solution interface. The inhibitor efficiencies obtained with Co(II) TCPC and Fe(III) TCPC are 68.5% and 82.4% respectively. Pre-etching the surface followed by coating with Fe(III) TCPC polymer gave an inhibitor efficiency of 73.5%, which is lower than that on an unetched surface.

Figure 6 shows the Bode plot for mild steel in 1% NaCl (pH = 2) in the presence of a single polymer coating of Fe(III) TCPC. Clearly, the Bode plot indicates the presence of only one relaxation, as confirmed by the single maximum in the phase angle data. However, at low frequencies a diminished relaxation associated with the corrosion process appears to be involved.

Figure 7 compares the Nyquist plots for mild steel with a single polymer coating of low-void-fraction Fe(III) TCPC containing p-hydroxy-pyridine groups in the voids against Fe(III) TCPC. Clearly, the R_p value in this case is lower than the 238.6 Ω cm^2 obtained with a polymer coating of Fe(III) TCPC, contrary to the expected increase in R_p. We

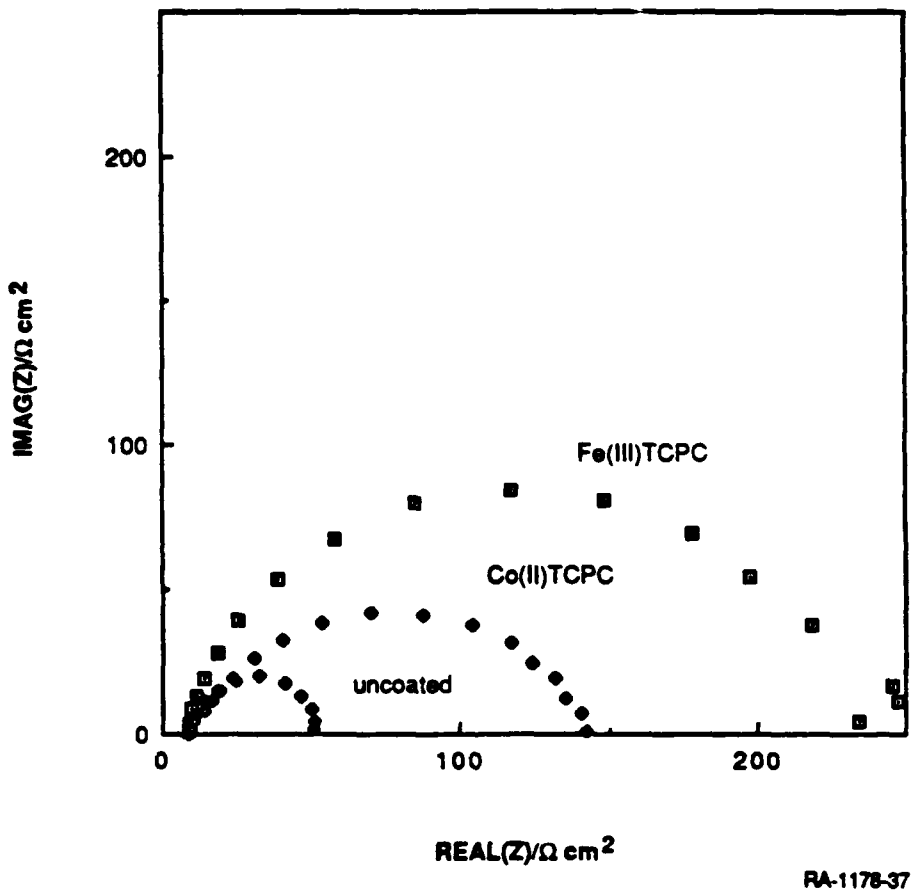

Figure 5. Nyquist plot for steel with and without Co(II) and Fe(III)TCPC. 1% NaCl solution; pH = 2; T = 298 K; 255 rpm.

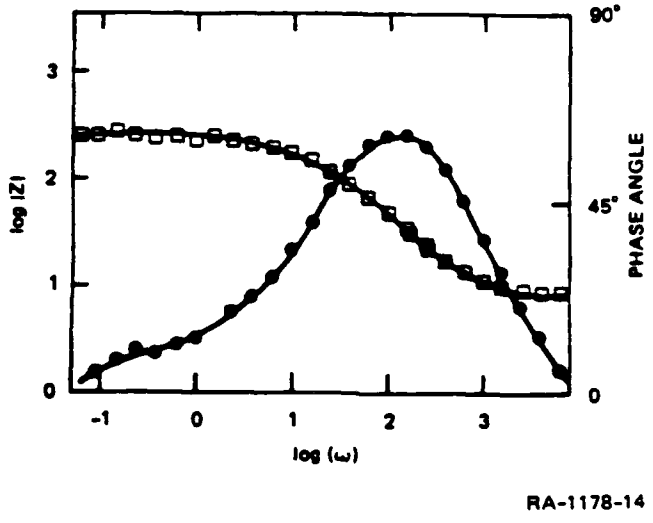

Figure 6. Bode plot for steel with one coat of Fe(III)TCPC.
1% NaCl solution; pH = 2; T = 298 K; 255 rpm

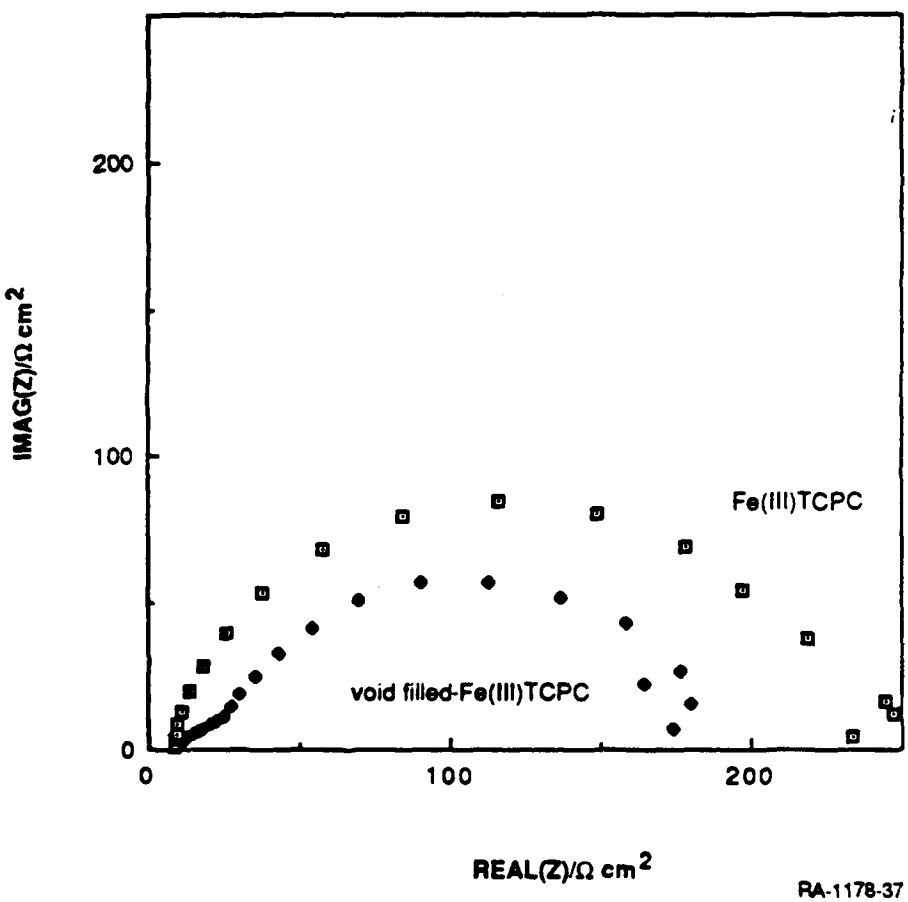

Figure 7. Nyquist plot for steel with Fe(III)TCPC and void-filled Fe(III)TCPC coatings.
1% NaCl solution; pH = 2; T = 298 K; 255 rpm.

attribute this lower value to the poor coverage of the metal surface by the polymer during its derivatization on the metal surface. An alternative approach would be to prepare the appropriately derivatized monomer first and then polymerize it on the metal surface to obtain the polymeric Fe(III) TCPC containing p-hydroxy pyridine groups in the voids. AC-impedance data of polymeric phthalocyanines are summarized in Table 3.

We also performed AC-impedance measurements of some of the polymeric and monomeric coatings prepared from Zn(II), OV(IV), Cr(III), and Si(IV) TCPCs and TCAUPCs. The results appear to show that some metal ion centers do not enhance inhibition activity whereas others do.

Figures 8 through 10 show Nyquist plots of CrIII) TCPC, Si(IV) TCPC and Zn(II) TCPC coated steel specimens tested in 1% NaCl (pH = 2). Clearly, the inhibition efficiency is not as good as that obtained with Fe(III) TCPC polymers. Preliminary investigation with Zn(II) TCAUPC indicates the formation of a stable corrosion-resistant coating because of the difficulty in obtaining an ohmic contact. We were able to make an ohmic contact to the metal only after vigorous removal of the coating with a coarse silicon carbide paper.

Slow Potentiodynamic Studies on Steel. Potentiodynamic polarization curves for mild steel in 1% NaCl solution (pH = 2) with and without polymer coatings are shown in Figure 11. A number of distinctive features appear in this figure, depending on the type of coating and the surface pretreatment of the metal. The corrosion potential for the system shifted toward more positive values with Co(II) TCPC, etched Fe(III) TCPC, and Fe(III) TCPC in that order. Fe(III) TCPC polymer coating appears to inhibit the cathodic reaction by almost a half order of magnitude, while the same coating inhibits the anodic reaction by almost two orders of magnitude up to about -450 mV (SCE). At potentials more positive than -450 mV (SCE), the polarization curves with and without coating appear to merge.

Another interesting feature of the diagram is the appearance of a relatively sharp rise in current at about -465 mV (SCE). This feature was completely absent in the case of uncoated steel. Thus, we can conclude that the sharp rise in current at -465 mV (SCE) is associated with the presence of the coating. Because the coating appears to remain intact at these positive potentials, the increase in current could be due to desorption of some adsorbed species at the pores of the coating. The desorption exposes the underlying metal to the environment and the anodic current rises accordingly.

The Fe(III) TCPC coating shows an inhibitor efficiency of 82%, the highest achieved among the polymeric macrocyclics of the porphyrin and phthalocyanine type. This finding is in excellent agreement with the AC-impedance data listed in Table 3. No beneficial effect toward inhibition was found by preetching the sample. Furthermore, the Fe(III) TCPC coating afforded better corrosion protection than the polymer coating of Co(II) TCPC.

Table 3

SUMMARY OF THE AC-IMPEDANCE DATA FOR MILD STEEL IN 1% NaCl SOLUTION (pH = 2) WITH AND WITHOUT POLYMER COATINGS

System	R_p (Ω cm^2)	ω_{max} (rad/ s)	C_p ($\mu F/cm^2$)	Inhibitor Efficiency (%)
S: 1% NaCl (pH = 2)	42.1	62.8	378	--
Mild steel with Co(II) TCPC (3 coatings)	133.6	9.96	752	68.5
Mild steel with Fe(III) TCPC coating	238.6	15.8	265	82.4
Etched steel with Fe(III) TCPC coating	158.6	15.8	399	73.5
Mild steel with low void fraction Fe(III) TCPC coating	174	1.58	3,661	77
Mild steel with Zn(II) TCPC coating	173	62.8	92	76
Mild steel with Cr(III) TCPC coating	88	0.628	18,095	52
Mild steel with Si(IV) TCPC coating	117.8	1.58	5,373	64

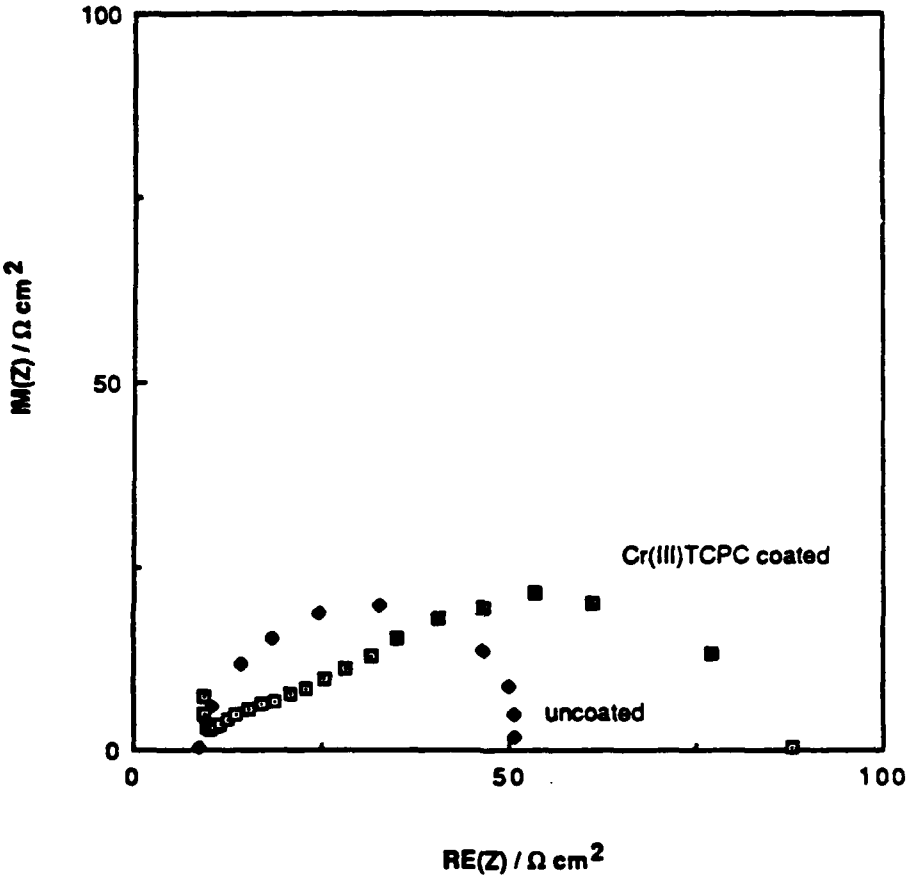

Figure 8. Nyquist plot for Cr(III)TCPC coated steel.
1% NaCl solution; pH = 2; T = 298 K; 255 rpm.

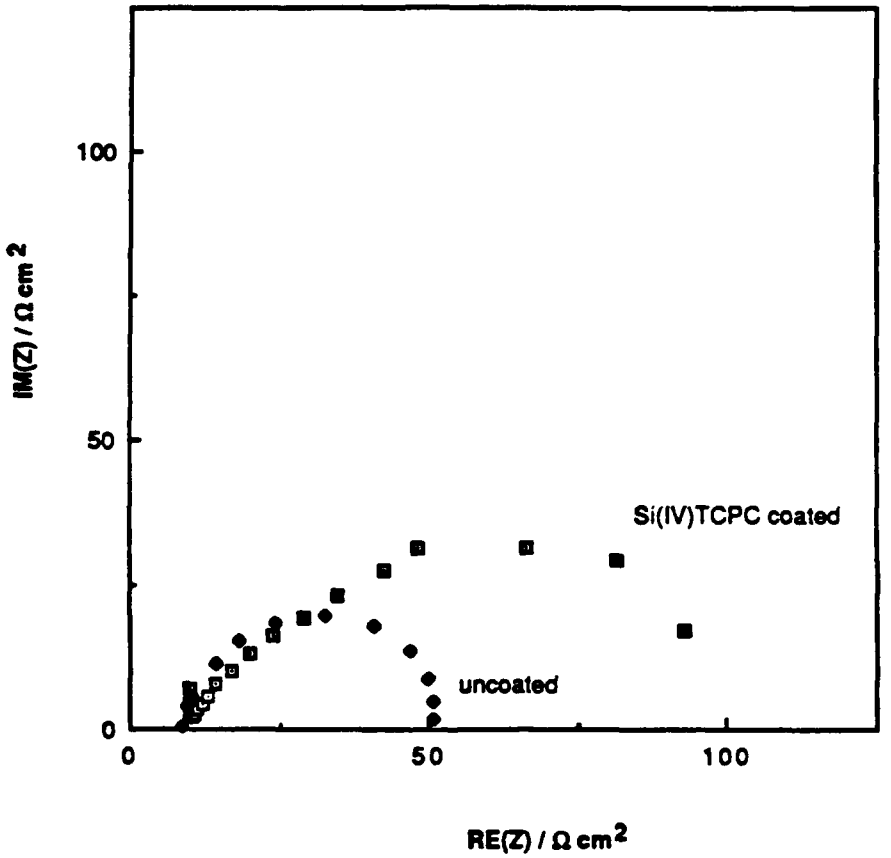

Figure 9. Nyquist plot for Si(IV) TCPC coated steel.
1% NaCl solution; pH = 2; T = 298 K; 255 rpm.

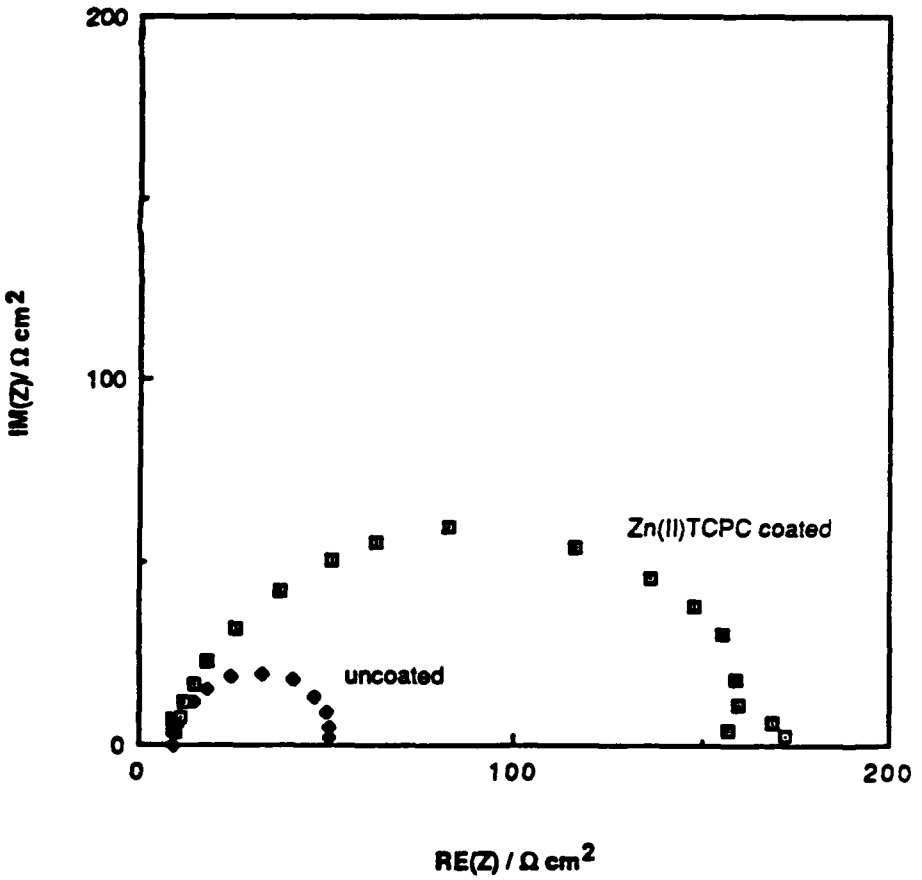

Figure 10. Nyquist plot for Zn(II)TCPC coated steel.
1% NaCl solution; pH = 2; T = 298 K; 255 rpm.

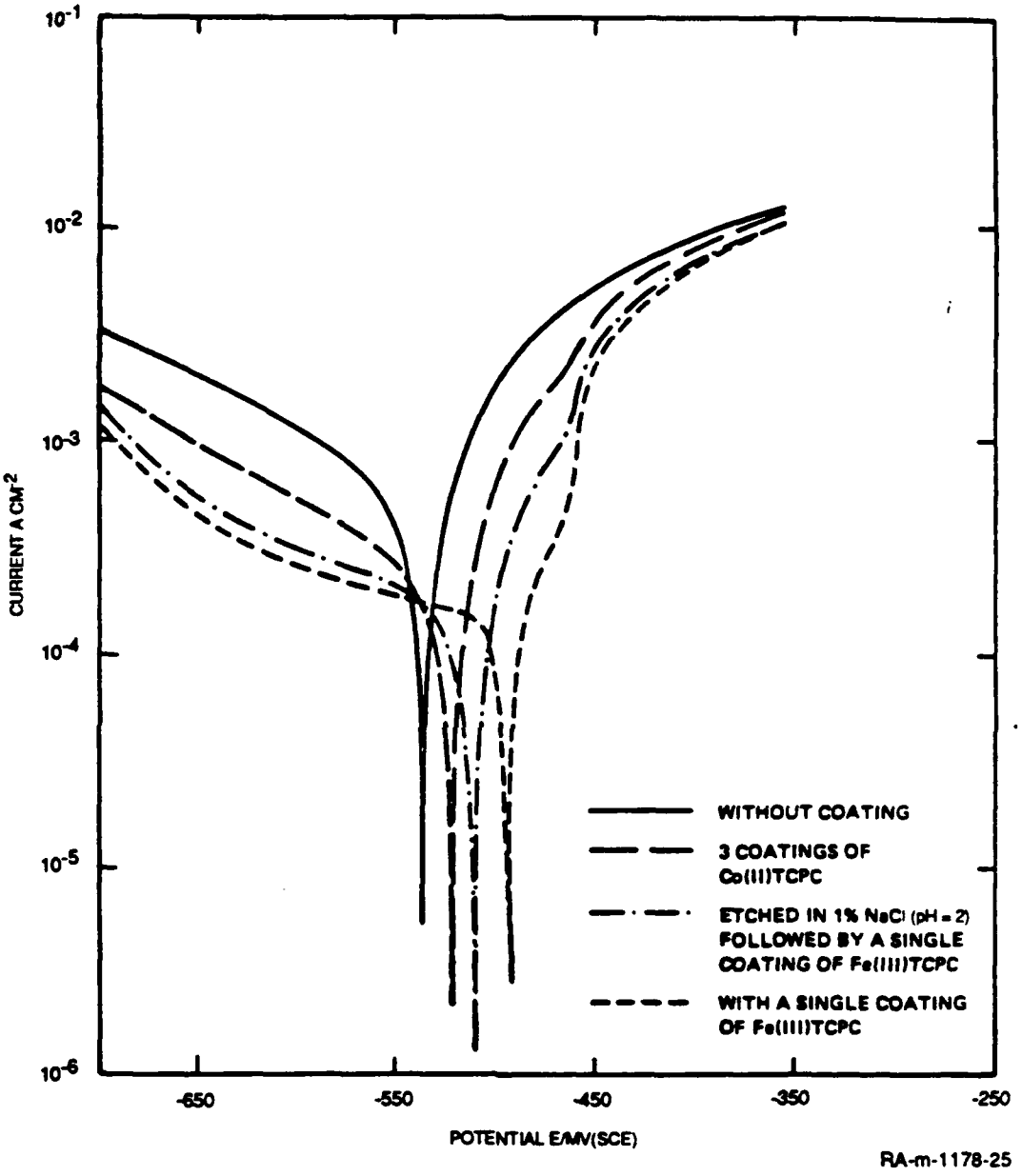

Figure 11. Current density-potential curves for steel with polymeric phthalocyanine coatings.

($|dE/dt| = 0.1$ mV s^{-1})
System: Mild steel/1% NaCl; pH = 2; 255 rpm; T = 298K.

Table 4 summarizes the slow potentiodynamic data for steel in 1% NaCl solution (pH = 2) with and without polymer coatings.

Surface Morphological Studies of Steel Coated with PhthalocyaninePolymers and Monomers. Figure 12 shows the scanning electron micrographs (SEMs) of the polyphthalocyanine-coated metal and the unpolymerized-phthalocyanine-coated metal at various magnifications. The unpolymerized coating clearly shows a "mud crack" type of appearance whereas the polymerized coating does not show evidence of such cracks. A close examination of the monomeric and polymeric coating at a magnification 5000X shows the fine-grained uncracked structure of the polymer compared with the coarse-grained cracked structure of the monomer. The uniform coverage of the metal by the polymer is clearly evident at 100X magnification. The white patches observed on the micrographs on polymerized as well as on unpolymerized samples are the excess material retained on the surface as a result of dip coating the sample. The conducting nature of the monomeric as well as the polymeric material is substantiated by the absence of any surface charging caused by the electron beam.

Long-Chain Derivatized Phthalocyanines

Synthesis

The tetracarboxyphthalocyanines were converted to the acid chlorides by refluxing with thionyl chloride, as shown in reaction 2. The tetra-acid chlorides (PCCOCl) were treated with an amino acid containing a long aliphatic chain (either 11-aminoundecanoic acid or 6-aminocaproic acid) to give the long-chain derivatized phthalocyanines, as shown in reaction 3. Six metal ions were used for these studies: including Co(II), Fe(III), Zn(II), OV(IV), Cr(III), and Si(IV).

Corrosion Studies

Figures 13 and 14 show the effect of incorporating long-chain hydrocarbon groups into the phthalocyanine molecule on the corrosion inhibition of steel. Figure 13 shows the Nyquist plots for steel in 1% NaCl (pH = 2) with Fe(III) and Co(II) tetrakis (N-carboxyl-12-aminoundecanoic acid) phthalocyanine (TCAUPC), respectively, both containing four 10-carbon aliphatic chains as shown in Figure 4. Note that Fe(III) TCAUPC shows an inhibition efficiency of approximately 88% whereas Co(II) TCAUPC shows an efficiency of 84%. In both instances the efficiency is greater than that obtained with the polyphthalocyanine coatings. We consider this to be a significant finding because the heat treatment in this case is performed at a much lower temperature (100°C-110°C) compared with the heat treatment of 450°C required for the polyphthalocyanine formation. The lower heat treatment required with long-chain hydrocarbon phthalocyanines prevents any undesirable structural weaknesses being thermally induced in the metal. Figure 14 shows the effect of Fe(III) and Co(II) tetrakis (N-carboxyl-6-amino-caproic acid)-phthalocyanine (TCACPC) on the Nyquist plot for steel in

Table 4

SUMMARY OF THE SLOW POTENTIODYNAMIC DATA FOR STEEL IN 1% NaCl SOLUTION (pH = 2) WITH AND WITHOUT POLYMER COATINGS

System	E_{corr} [mV vs (SCE)]	b_a (mV/decade)	b_c (mV/decade)	I_{corr} (A/ cm^2)	Inhibitor Efficiency (%)
S: 1% NaCl, pH = 2	-538	247	-193	4.75×10^{-4}	--
Steel with Co(II) TCPC (3 coatings)	-523	257	-204	2.2×10^{-4}	54
Steel with Fe(III) TCPC coating	-493	224	—	8.5×10^{-5}	82
Etched steel with Fe(III) TCPC coating	-512	228	—	1.6×10^{-4}	66

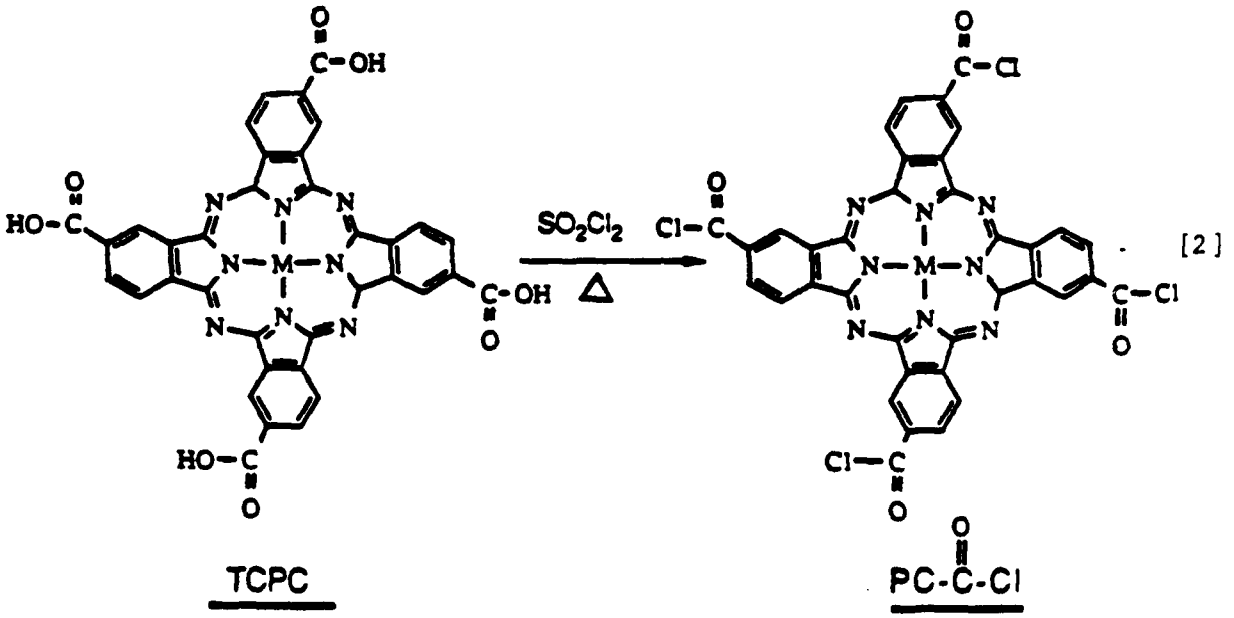
HO-C
C-OH
SO_2Cl_2
Cl-C
C-Cl
TCPC
PC-C-Cl

[2]


PC-C-Cl + H_2N-R-C-OH
NaOH
PC-C-N-R-C-OH + HCl

[3]

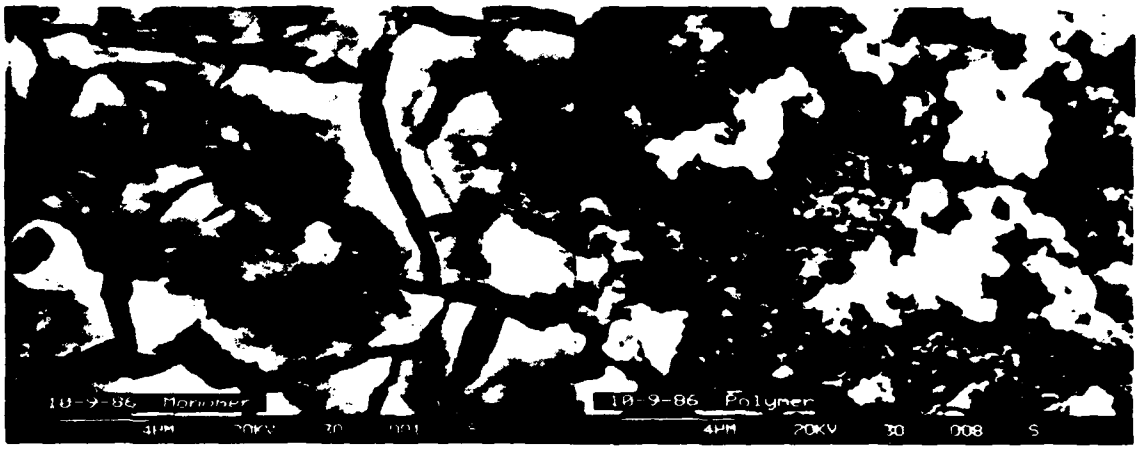

5000 X

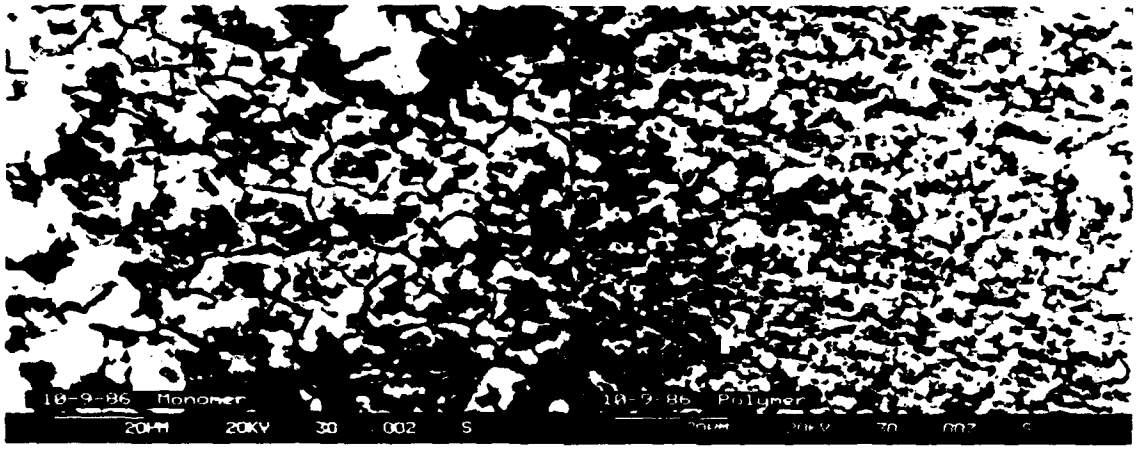

1000 X

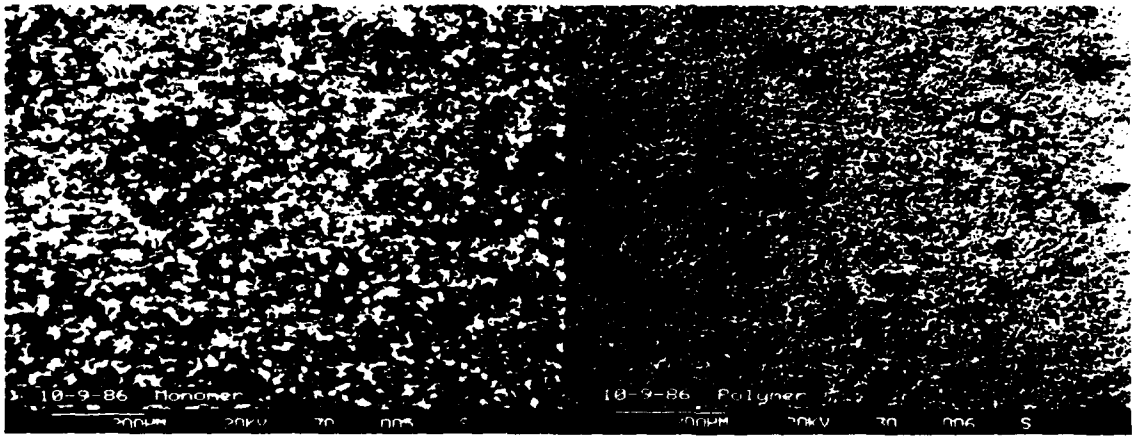

100 X

RA-m-1178-5

Figure 12. Comparison of the surface morphology of monomeric and polymeric Fe(III)TCPC coatings at different magnifications.

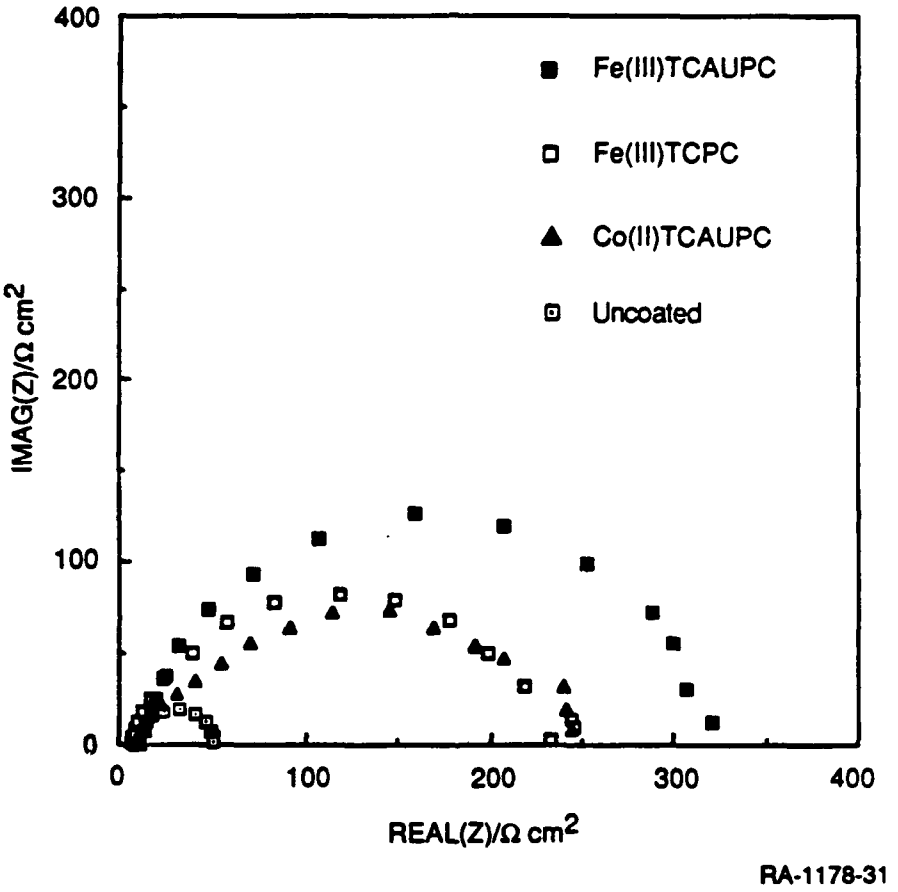

Figure 13. Comparison of the Nyquist plots of Fe(III)TCPC coated and ten carbon alkyl chain containing phthalocyanine-coated steel.
Mild steel: 1% NaCl; pH = 2; T = 298 K; 255 rpm.

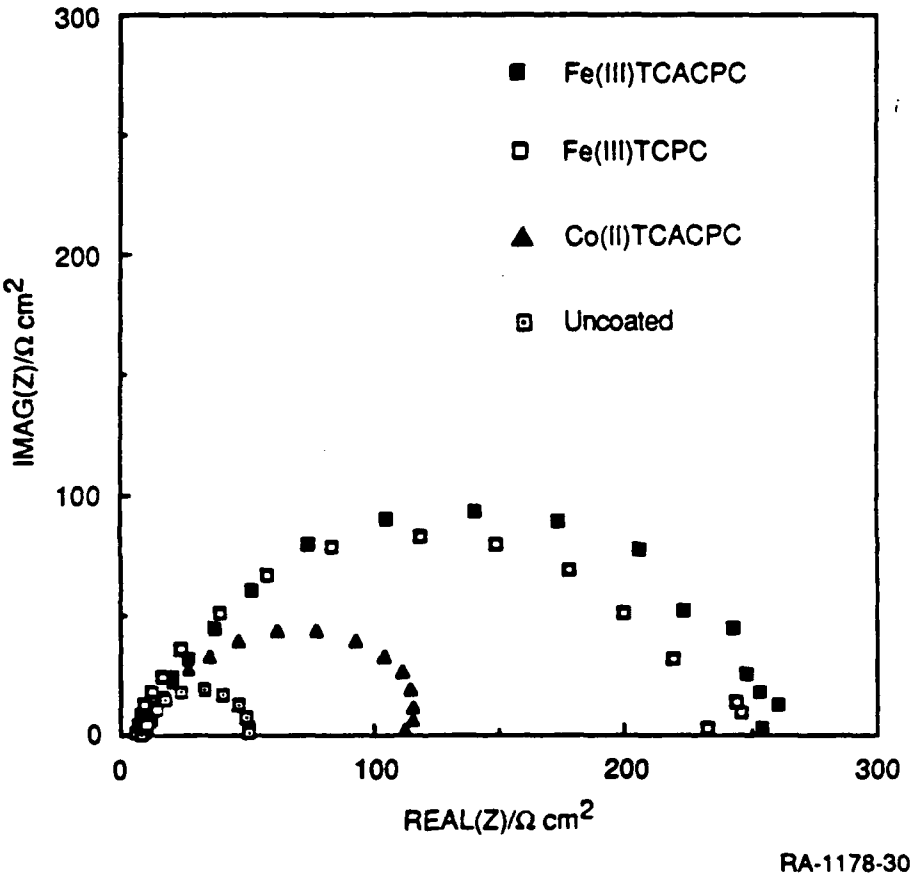

Figure 14. Comparison of the Nyquist plots of Fe(III)TCPC coated and five carbon alkyl chain containing phthalocyanine-coated steel.
Mild steel: 1% NaCl; pH = 2; T = 298 K; 255 rpm

the same solution. Once again, Fe(III) TCACPC shows greater inhibition efficiency (84%) than its Co(II) counterpart.

Table 5 summarizes the AC-impedance data for mild steel in 1% NaCl (pH = 2) with and without monomer and polymer coatings.

In a future study we hope to investigate the application of TCACPC and TCAUPC coatings onto both steel and aluminum surfaces treated with aminopropyl-triethoxysilane. We believe that the ability of silanes to bind to surfaces containing hydroxyl groups will provide a better binding surface for TCACPC and TCAUPC than the untreated metal surfaces. Figures 15 and 16 show the degree of inhibition provided by Co (II) and Fe (III) centered TCACPC and TCAUPC coatings, respectively. Clearly, from the polarization curves, both anodic and cathodic reactions are inhibited by these coatings. The degree of inhibition of the anodic reaction is greater than that of the cathodic reaction in both cases, thereby shifting the corrosion potential in the anodic direction. Moreover, Fe (III) TCACPC coating, which provides greater inhibition, shifts the corrosion potential in the anodic direction by a greater amount than the Co (II) TCACPC coating, which inhibits corrosion to a lesser extent, thereby shifting the corrosion potential by a smaller amount.

The electrochemical parameters obtained from Figures 15 and 16 are summarized in Tables 6 and 7, respectively. Clearly, the corrosion inhibition efficiencies evaluated from the polarization data are lower than those derived from the impedance analysis. This discrepancy most likely exists because the AC-impedance data are generated around the corrosion potential, whereas the evaluation of I_{corr} and hence the inhibition efficiency requires a much greater system perturbation into the Tafel regions.

The large potential perturbations appear, to affect the TCACPC and TCAUPC coatings more than the TCPC coatings, possibly because the former are not polymers whereas the latter are. Because the polymer TCPC is more strongly bound onto the metal surface than the monomers TCACPC and TCAUPC, the inhibition efficiency is not affected by its mode of evaluation (i.e., by AC-impedance analysis or by polarization diagrams). TCACPC and TCAUPC, however, are probably not strongly bound in the anodic region, thereby exhibiting higher currents than the TCPC polymer coated surface (Figures 15 and 16). Thus, if the system is prone to polarization effects, the inhibition efficiencies obtained by polarization data are more realistic.

Corrosion Inhibitors on Aluminum

Synthesis

Previous studies showed that the phthalocyanine complexes are not very effective in protecting aluminum-7075 alloy from corrosion, probably because the phthalocyanine is not very adhesive to the aluminum surface. Unlike iron, aluminum is not a good π electron acceptor. In

Table 5

SUMMARY OF THE AC-IMPEDANCE DATA FOR MILD STEEL IN 1% NaCl SOLUTION (pH = 2) WITH AND WITHOUT COATINGS

System	R_p (Ω cm^2)	ω_{max} (rad/s)	C_p ($\mu F/cm^2$)	Inhibitor Efficiency (%)
S: 1% NaCl, (pH = 2)	42.1	62.8	378	--
Mild steel with Fe(III) TCPC coating	238.6	15.8	266	82.4
Mild steel with Fe(III) TCAUPC coating	323.4	15.8	196	87.6
Mild steel with Co(II) TCAUPC coating	243.1	3.96	1038	83.5
Mild steel with Fe(III) TCAPC coating	255	25	156.7	84
Mild steel with Co(II) TCAPC coating	113.8	39.6	221.6	65
Mild steel with Zn(II) TCAUPC coating	332.6	6.28	479	87

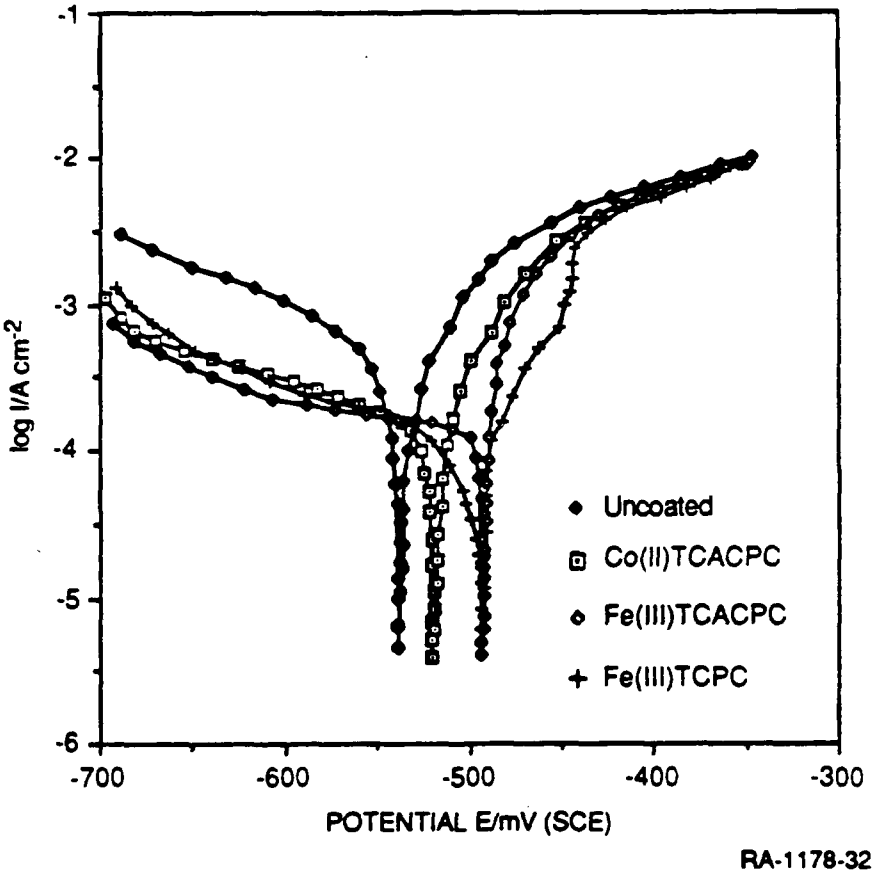

Figure 15. Current density-potential curves for mild steel with coatings having five carbon alkyl chain containing phthalocyanines.

($dE/dt = 0.1\ mV\ s^{-1}$)
Mild steel: 1% NaCl; pH = 2; T = 298K; 255 rpm.

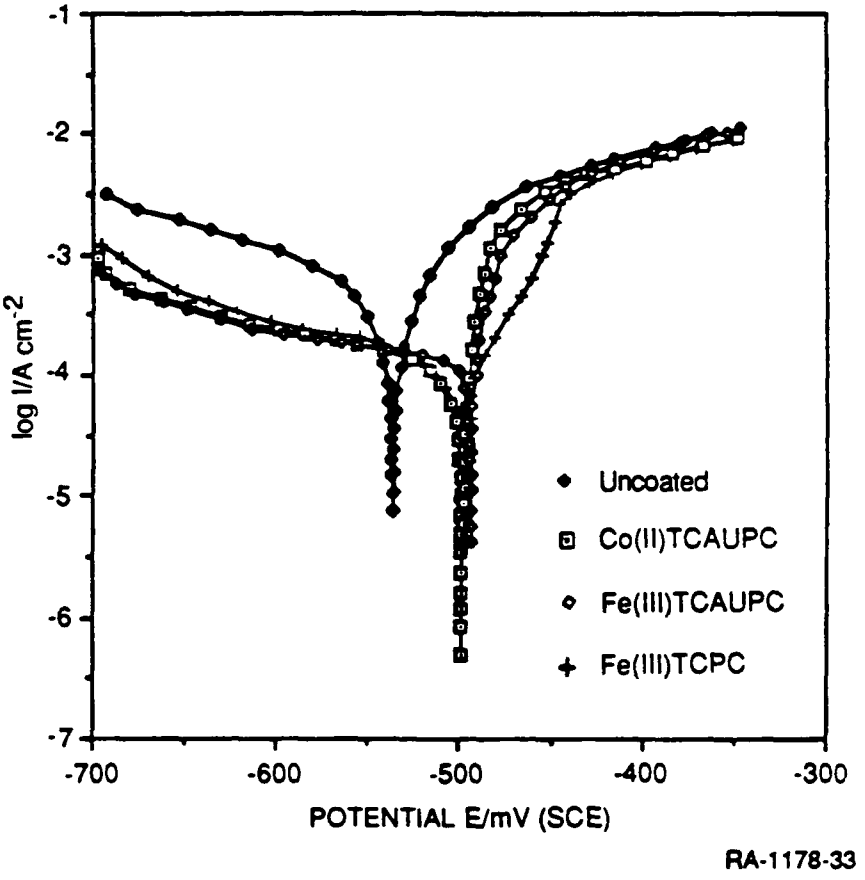

Figure 16. Current density-potential curves for mild steel with coatings having ten carbon alkyl chain containing phthalocyanines.
($dE/dt = 0.1\ mV\ s^{-1}$)
Mild steel: 1% NaCl; pH = 2; 255 rpm; T = 298 K.

Table 6

A COMPARISON OF THE SLOW POTENTIODYNAMIC DATA FOR STEEL IN 1% NaCl SOLUTION (pH = 2) WITH AND WITHOUT FIVE CARBON ALKYL CHAIN CONTAINING PHTHALOCYANINE COATINGS AGAINST POLY Fe(III) TCPC COATINGS

System	E_{corr} [(mV vs (SCE)]	b_a (mV/decade)	b_c (mV/decade)	I_{corr} (A/cm^2)	Inhibitor Efficiency (%)
S: 1% NaCl, pH = 2	-538	247	-193	4.75×10^{-4}	--
Steel with Fe(III) TCPC coating	-493	224	--	8.5×10^{-5}	82
Steel with Co(II) TCACPC coating	-518	254	--	1.7×10^{-4}	64
Steel with Fe(III) TCACPC coating	-496	250	-272	1.55×10^{-4}	67

Table 7

A COMPARISON OF THE SLOW POTENTIODYNAMIC DATA FOR STEEL IN 1% NaCl SOLUTION (pH = 2) WITH AND WITHOUT TEN CARBON ALKYL CHAIN CONTAINING PHTHALOCYANINE COATINGS AGAINST POLY Fe(III)TCPC COATINGS

System	E_{corr} [mV vs (SCE)]	b_a [mV/decade)	b_c (mV/decade)	I_{corr} (A/cm^2)	Inhibitor Efficiency (%)
S: 1% NaCl, pH = 2	-538	247	-193	4.75×10^{-4}	--
Steel with Fe(III) TCPC coating	-493	224	—	8.5×10^{-5}	82
Steel with Co(II) TCAUPC coating	-500	265	—	1.3×10^{-4}	73
Steel with Fe(III) TCAUPC coating	-497	226	—	1.35×10^{-4}	72

our previous work with aluminum, we found that silane derivatives strongly bind to the aluminum surface by formation of Si-O-Al covalent bonds with the oxide coating at the aluminum surface. Therefore, we decided to synthesize a long-chain phthalocyanine having silane groups attached to one end of the hydrocarbon chain. In the first strategy, the silane precursor is coated on the aluminum surface and then reacted with a phthalocyanine derivative according to reaction 4. The coating was subsequently heat treated at 450°C.

Corrosion Studies

AC-Impedance Studies on Aluminum-7075. The Nyquist plot for aluminum-7075 alloy in 1% NaCl solution (pH = 2) in the absence of any inhibitor or polymer coating is shown in Figure 17. The impedance diagram clearly consists of three distinct regions: an initial time constant involving the relaxation of the oxide dielectric at high frequencies, a Warburg type diffusional impedance possibly involving diffusing species responsible for oxide growth, and low-frequency relaxation involving the film/solution interface. The R_p value for interfacial impedance is 209 Ω cm^2 and the corresponding capacitance is 1209 μF/cm^2 because of the presence of the stable Al_2O_3 film on the aluminum surface.

The Nyquist plot for aluminum-7075 in the same solution with three polymer coatings of Co(II) TCPC is shown in Figure 18. The most striking difference between Figures 17 and 18 is the drastic reduction of R_p in the presence of Co(II) TCPC. In addition, the initial high frequency relaxation observed in Figure 17 due to the Al_2O_3 film has also disappeared from Figure 18. The Co(II) TCPC polymer coating has either prevented or inhibited the formation of the Al_2O_3 film, thereby giving rise to higher corrosion rates. The R_p and C_p values for the coated aluminum are 35.5 Ω cm^2 and 180 μF/cm^2, respectively. The Rp value has thus been reduced by almost six times, activating the corrosion of the metal by the same degree, provided no change occurs in the Tafel slopes.

Figure 19 shows the Nyquist plot for etched aluminum-7075 coated with octadecyltrichlorosilane (ODTCS) by heat treatment at 110°C. The concept we adopted here was first to produce a grainy surface with a porous aluminum oxide film. The treatment of the oxide with ODTCS creates an Al-O-Si linkage at the aluminum oxide surface such that the hydrophobic octadecyl group projects from the aluminum surface. Thus, this treatment renders the aluminum surface strongly hydrophobic, thereby causing a tremendous reduction in its corrosion rate. We also believe that the silane treatment will enable better binding of the phthalocyanine onto the aluminum surface.

Experiments performed by reacting the silane precursor treated aluminum surface with the phthalocyanine derivative (reaction 4) and subsequent treatment did not give good results, probably because of the cleavage at the amide linkage. We believe that a low temperature treatment of the coating will be beneficial in this case.

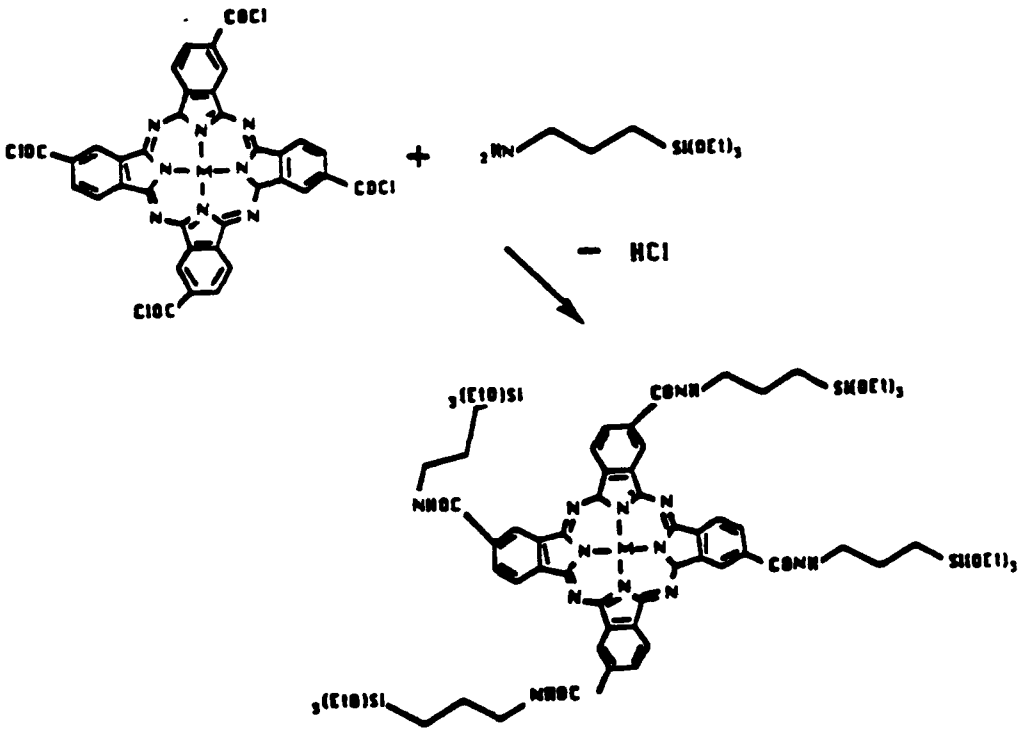
COCl
ClOC
COCl
ClOC
+
$_2$HN
Si(OEt)$_3$
– HCl
$_3$(EtO)Si
NHOC
CONH
Si(OEt)$_3$
CONH
Si(OEt)$_3$
$_3$(EtO)Si
NHOC

[4]

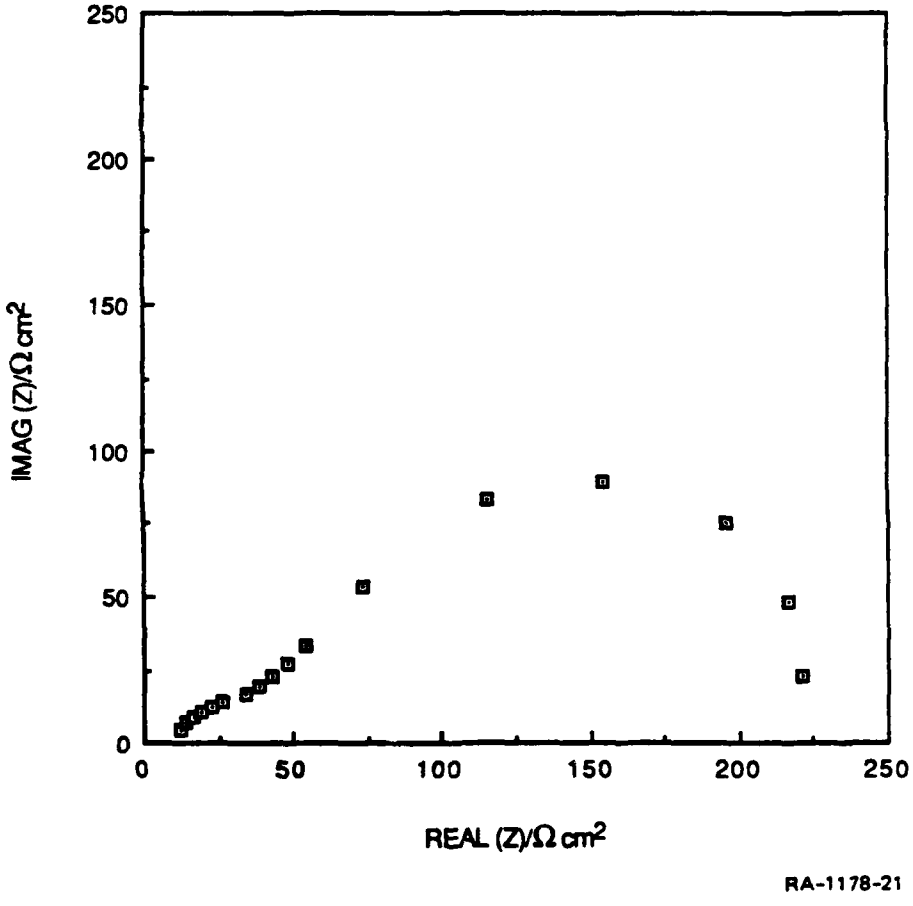

Figure 17. Nyquist plot for uncoated Al-7075 alloy.
1% NaCl solution; pH = 2; T = 298 K; 255 rpm.

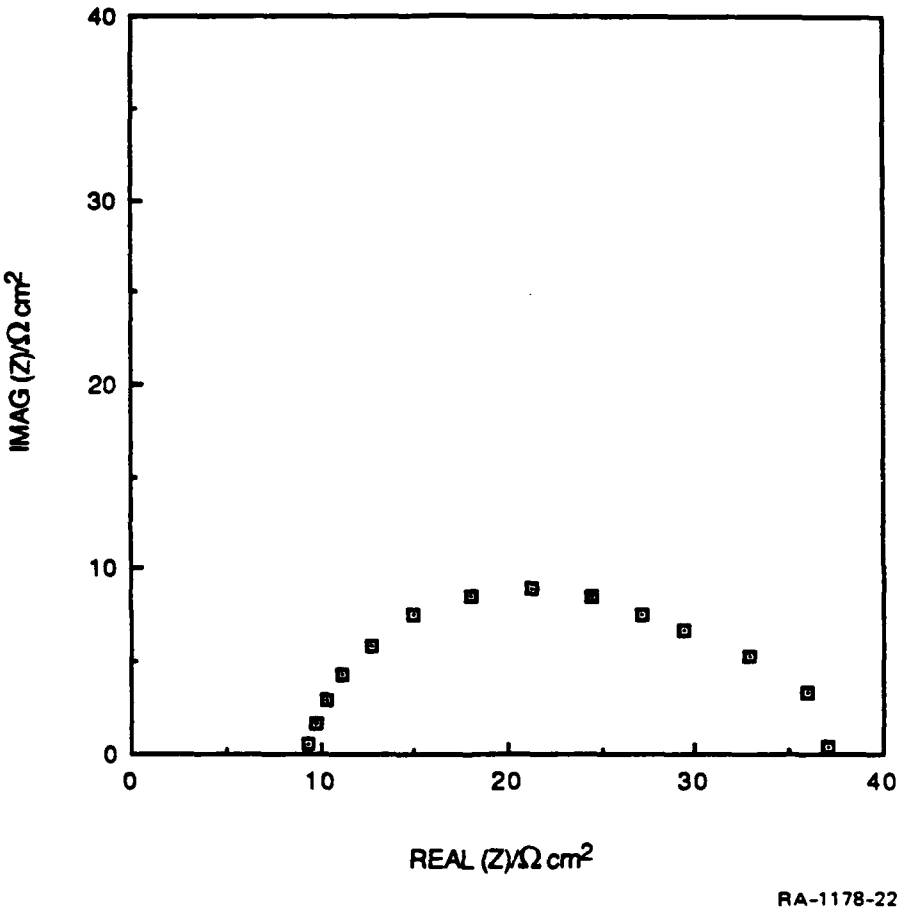

Figure 18. Nyquist plot for Al 7075 with three coats of Co(II)TCPC.
1% NaCl solution; pH = 2; T = 298 K; 255 rpm.

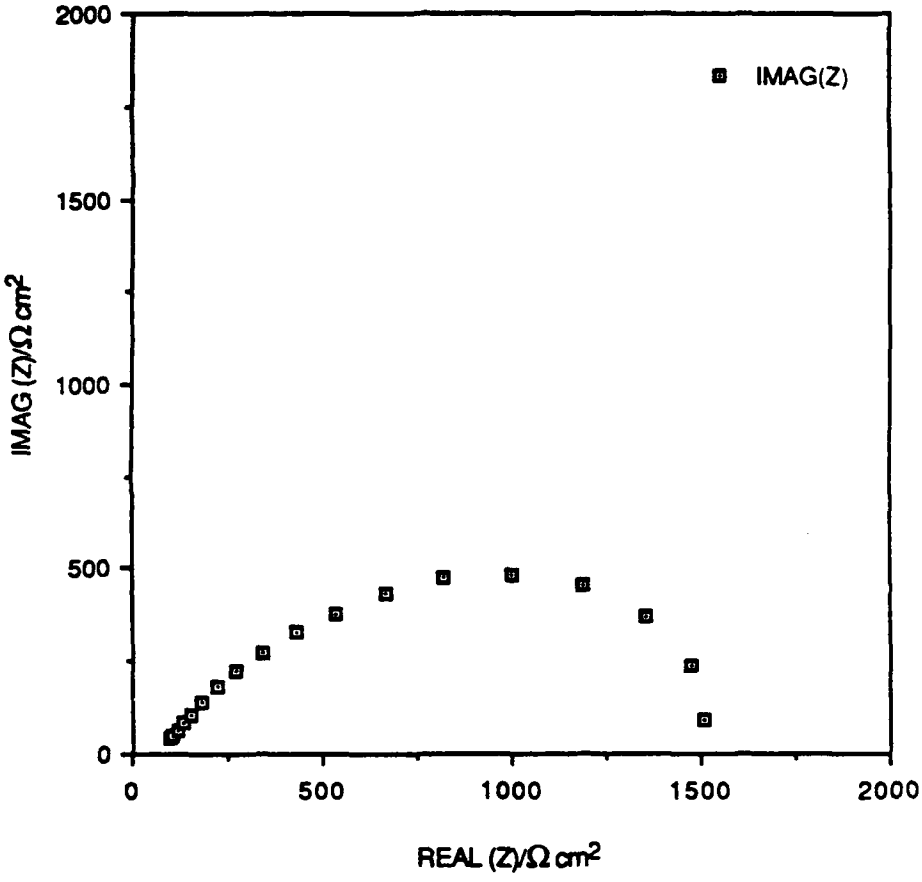

Figure 19. Nyquist plot for Al-7075 with one coat of ODTCS
1% NaCl solution; pH = 2; T = 298 K; 255 rpm.

Table 8 summarizes the AC-impedance data for aluminum-7075 alloy in 1% NaCl (pH = 2) with and without polymer coatings.

Slow Potentiodynamic Studies on Aluminum-7075. Potentiodynamic polarization curves for aluminum-7075 alloy in 1% NaCl solution (pH = 2) with and without polymer coatings are shown in Figure 20. Note that the aluminum-7075 alloy without any coating yields lower cathodic currents (almost by half an order of magnitude) than those with coatings. This event can be attributed to the formation of a stable protective oxide film of Al_2O_3 on the surface of the bare alloy. This finding is also confirmed by the AC-impedance data shown in Table 8, where the bare alloy exhibits large resistive and capacitive components. The formation of the polymer coating on the aluminum alloy has apparently prevented or inhibited the formation of the stable and protective Al_2O_3 film on its surface. Higher cathodic currents observed in the presence of the coating may be due to the interaction of the acidic environment generating hydrogen at the pores of the coating. Moreover, the oxide film at the pores does not appear to form, possibly because of the rapid transport of H^+ ions through the pores.

On the anodic branch, the currents without coating exhibited higher values compared with those with coatings. However, this effect was somewhat marginal and not as prominent as the difference observed on the cathodic branch.

Therefore, in general, the polymer coating formation activates the corrosion process even after a preetching treatment. We believe that the most beneficial means of obtaining high inhibition efficiencies with aluminum-7075 is first to form the stable protective Al_2O_3 film and thereafter bind a silane onto the hydrophilic surface. Because of the surface active property of the silane it is strongly adsorbed onto the surface with hydrophobic groups protruding ultimately blocking the surface of the pore base layer. This process has drastically reduced the corrosion of the aluminum alloy to a bare minimum.

Table 9 summarizes the slow potentiodynamic data for aluminum-7075 alloy in 1% NaCl solution (pH = 2) with and without polymer coatings.

Void-Filled Polymers

Synthesis

Examination of the structure of the polymeric phthalocyanine coatings (Figure 2) showed that they contained voids that would allow access of water molecules to the metal, thereby creating potential corrosion sites. We therefore considered that corrosion inhibition could be improved by filling the voids with organic molecules that potentially had corrosion-inhibiting properties themselves.

We attempted to fill the void by coupling hydroxypyridine groups to the aromatic ring of the phthalocyanine so as to fill the voids shown in

Table 8

SUMMARY OF THE AC-IMPEDANCE DATA FOR ALUMINUM-7075 ALLOY IN 1% NaCl SOLUTION (pH = 2) WITH AND WITHOUT POLYMER COATINGS

System	R_p (Ω cm^2)	ω_{max} (rad/s)	C_p ($\mu F/cm^2$)	Inhibitor Efficiency (%)
S: 1% NaCl (pH = 2)	209	3.96	1209	—
Al-7075 with Co(II) TCPC -(3 coatings)	35.3	157.8	180	<0
Etched Al-7075 with Co(II) TCPC coating	27.2	62.8	585	<0
Etched Al-7075 coated with ODTCS	1509	15.78	41.9	86

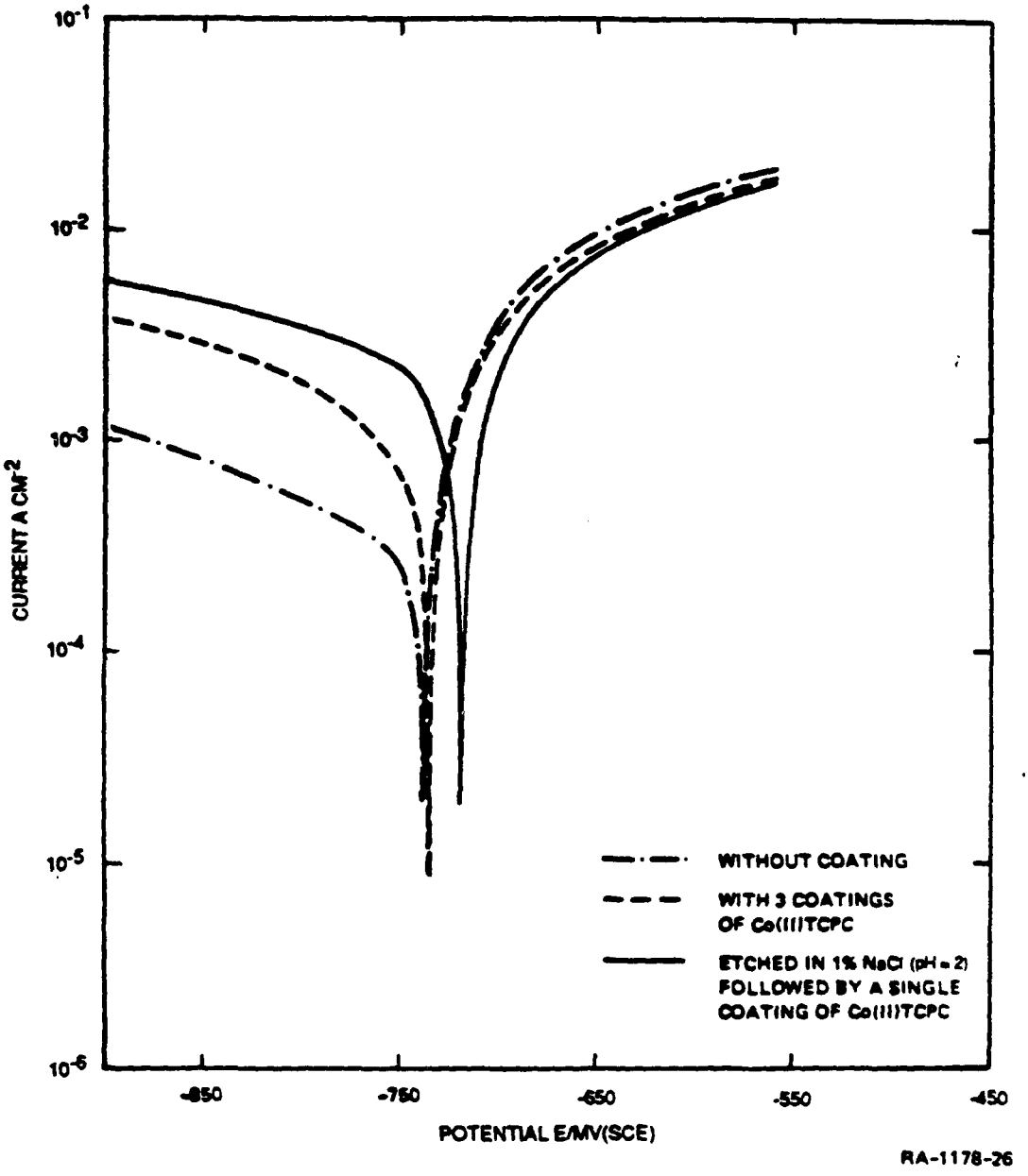

Figure 20. Current density-potential curves for Al-7075 with monomeric phthalocyanine coatings.
($|dE/dt| = 0.1$ mV s^{-1})
System: Aluminum-7075 Alloy/1% NaCl; pH = 2; 255 rpm; T = 298K.

Table 9

SUMMARY OF THE SLOW POTENTIODYNAMIC DATA FOR ALUMINUM-7075 ALLOY IN 1% NaCl SOLUTION (pH = 2) WITH AND WITHOUT POLYMER COATINGS

System	E_{corr} mV vs (SCE)	b_a [mV/decade)	b_c (mV/decade)	I_{corr} (A/cm^2)	Inhibitor Efficiency %)
S: 1% NaCl, pH = 2	-740	249	-254	2.86×10^{-4}	--
Al-7075 with Co(II) TAPC (3 coatings)	-736	--	-330	$1,3 \times 10^{-3}$	--
Etched Al-7075 CO(II) TCPC COATING	-720	--	-322	1.85×10^{-3}	--

Figure 3. Our first attempt at the coupling reaction was based on the work of Snow[6]; he coupled aromatic groups to phthalocyanines by a direct replacement reaction of aromatic nitro groups. We therefore attempted to make the tetranitro-tetracarboxyphthalocyanine to have both polymer-forming functionality and nitro-forming functionality for displacement. Direct nitration of the Fe(III) TCPC was unsuccessful because refluxing the phthalocyanine in nitric acid destroys the phthalocyanine ring. As an alternative, we took trimellitic anhydride (our starting material for TCPC synthesis) and nitrated it under rigorous nitrating conditions (as shown in reaction 5).

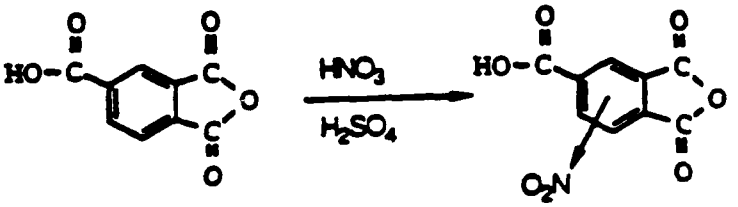

[5]

We checked the product of this reaction by IR spectroscopy, which was positive for nitro groups. We split the product in two and used one fraction in a phthalocyanine synthesis. The isolated nitrated tetra-carboxyphthalocyanine was then split into two fractions. The first was coated on steel samples and polymerized. The coated polymerized samples were then treated under the conditions required for the direct displace ment of nitro groups with oxypyridine groups. These samples did not show any improvement in corrosion inhibition. The second fraction of nitrated trimelliitic acid was treated with hydroxypyridine in basic DMSO, as shown in reaction 6.

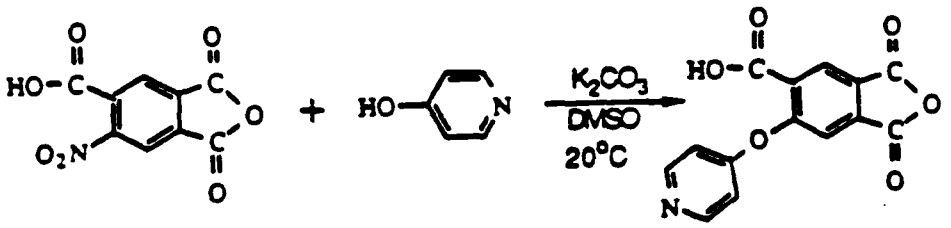

[6]

We were unable to isolate any product from this reaction. We believe that the coupling reaction did not occur because the acid groups of the tribenzoic acid interfered with the reaction. We could test this hypothesis by protecting the acid groups before the coupling reaction by converting the nitrated tribenzoic acid into phthalocyanine, which produce the two ortho acid groups. The third acid group from the nitrated tribenzoic acid is converted to an amide during the phthalo-cyanine synthesis; this amide is also an effective protecting group. Thus, the second fraction of the phthalocyanine made from the nitrated trimellitic acid was not hydrolyzed from the amide to the acid in the final synthesis step. We then tried the coupling reaction with the

material that had all the acid groups protected; nitrated tetraamidophthalocyanine was treated with hydroxypyridine in basic DMSO under the previously described conditions for direct displacement reactions (reaction 7). The product was considerably more soluble than the reactant. We therefore believe that the displacement reaction occurred.

At this point, we received the results of elemental analysis showing that only a small percentage of the nitration of trimellitic anhydride was proceeding. This result is not surprising since the carboxylic groups deactivate toward aromatic substitution reactions. We therefore performed the substitution on an aromatic ring with activating groups. Because methyl groups are activating, we attempted the aromatic substitution of trimethylbenzene. The overall synthesis strategy is shown in Figure 21.

Nitration of 1,2,4-Trimethylbenzene. The nitration of 1,2,4-trimethylbenzene was first attempted at room temperature using a slight excess of HNO_3, both with and without H_2SO_4. In both cases, the reaction mixture became extremely hot, evolved a red-brown gas (NO_2), and turned black. In one case, a small amount of a white, powdery solid was obtained in very poor yield. The NMR spectrum of this solid looked like the dinitration product. On the basis of the simple rules for aromatic substitution of benzene, we assumed that the product was 3,5-dinitro-1,2,4-trimethylbenzene.

The nitration was then attempted at ice-bath temperature using a slight excess of HNO_3, both with and without H_2SO_4. The reaction without H_2SO_4 showed little progress toward nitration after 45 min. The reaction with H_2SO_4 yielded a single product after 2 h, but when repeated on a large scale it provided a mixture of two major products. Vacuum distillation of the mixture provided the dinitrated compound as determined by NMR. Aliquots of a small-scale reaction were worked up at several time increments and showed that dinitration was occurring too quickly to make this combination of reagents a useful preparation of the mononitrated 1,2,4-trimethylbenzene. Nitration was attempted with HNO_3 in chloroform without success. The use of acetic anhydride as a solvent eliminated the problem of dinitration but led to the appearance of another side product. The NMR spectrum of this side product showed a peak consistent with acetylation of one of the ring methyl groups. Neither vacuum distillation nor flash chromatography could conveniently separate the desired nitro compound from the side product. This method was discontinued because of the large amount of side product formed.

We then decided to attempt to work with the dinitrotrimethylbenzene. Figure 22 shows the strategy for oxidation of the methyl groups to acid and then the substitution prior to the synthesis of the phthalocyanine.

Attempted Oxidation of 3,5-Dinitro-1,2,4-Trimethylbenzene. To form the substituted phthalocyanine, we would need the appropriate triacid. We wished to oxidize the 3,5-dinitro-1,2,4-trimethylbenzene with $KMnO_4$.

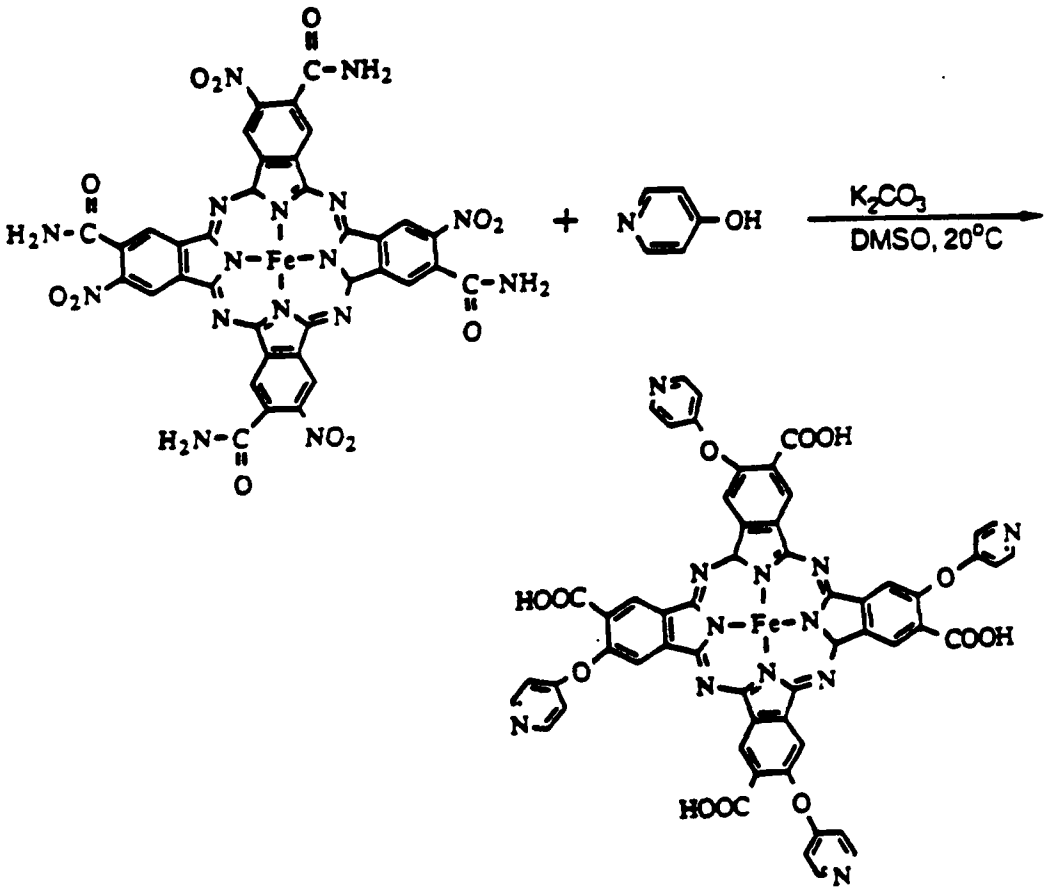

[7]

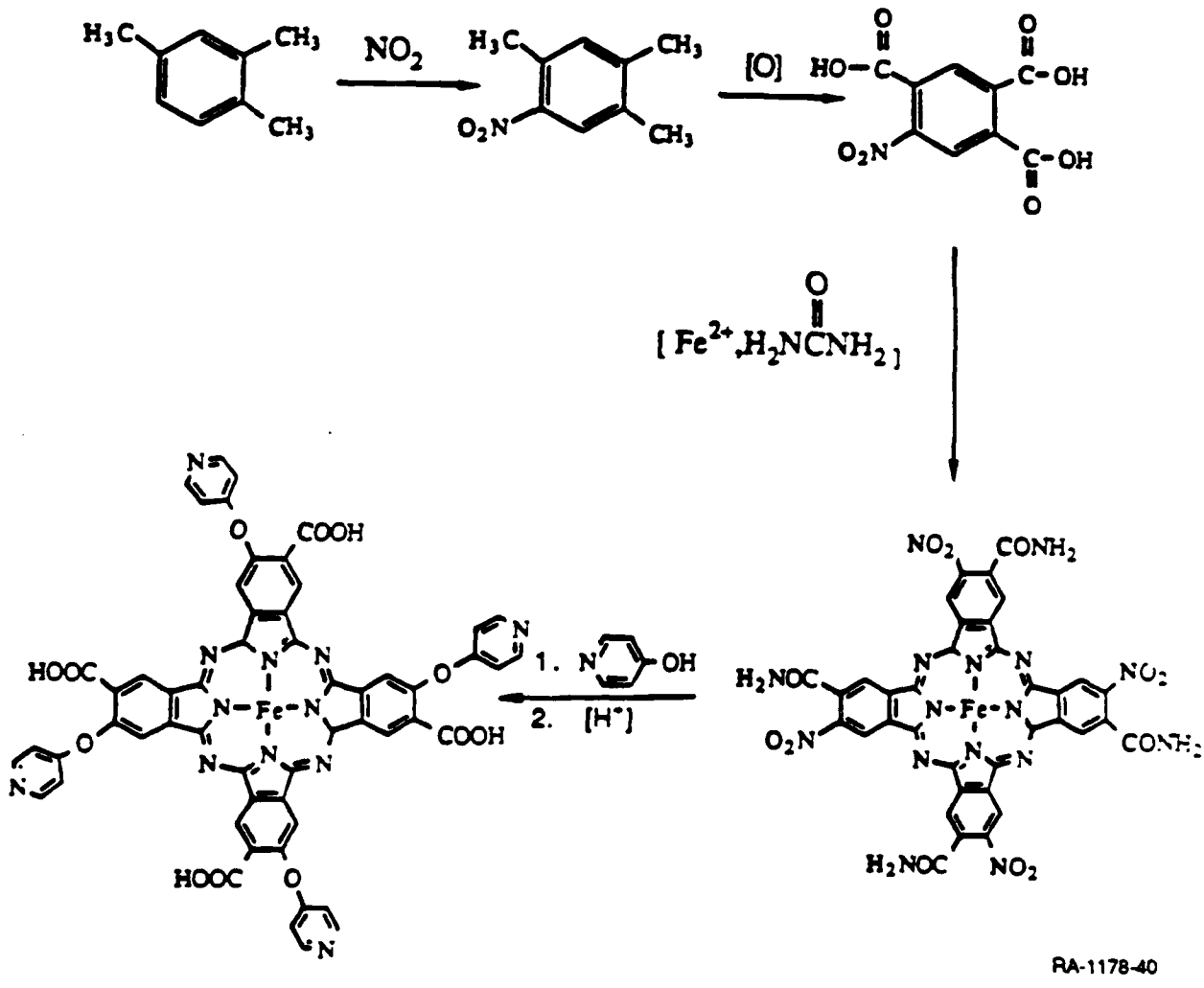

Figure 21. Synthesis of oxypyridine substituted FeTCPC.

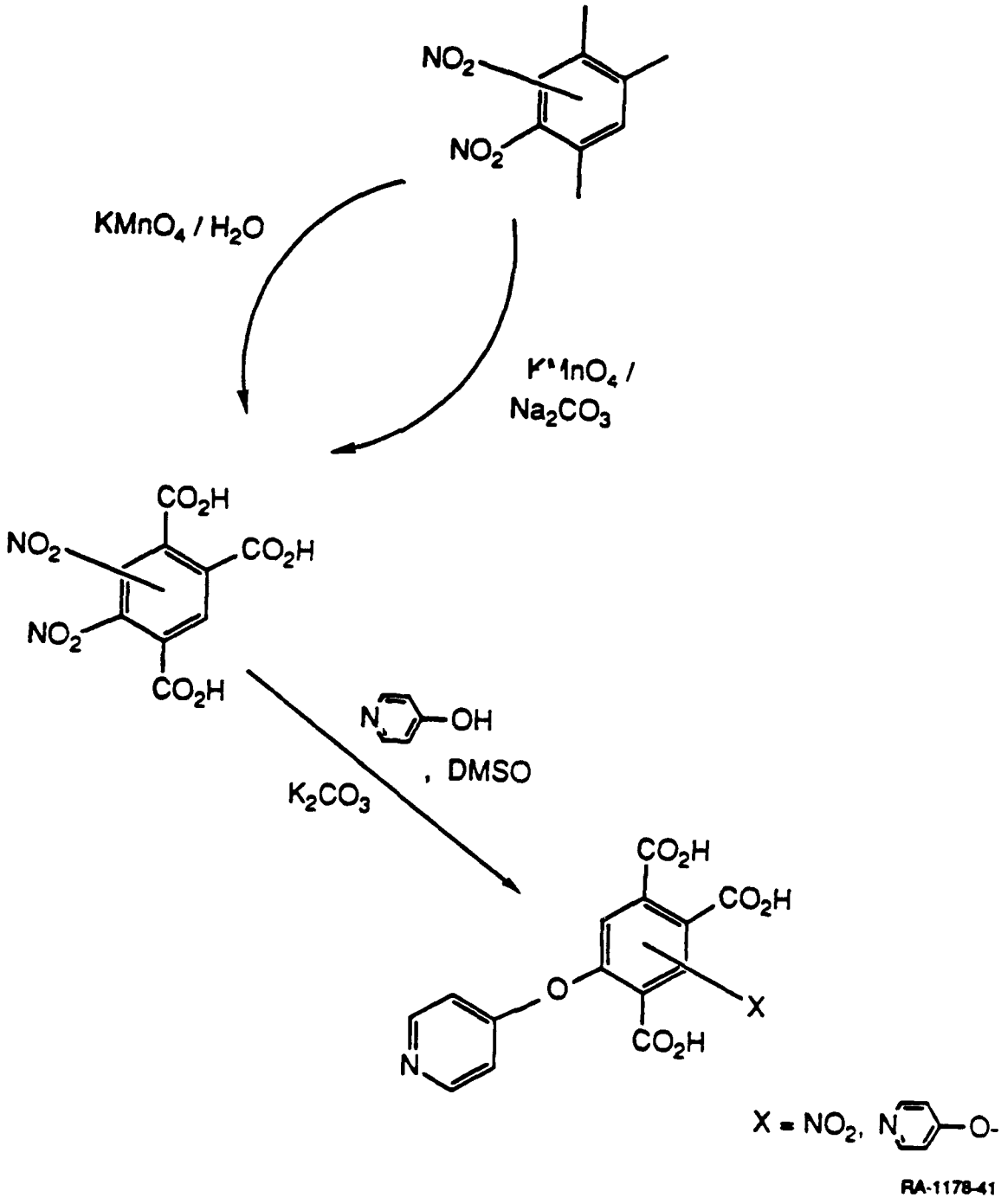

Figure 22. Oxidation of dinitrotrimethylbenzene to the dinitrotribenzoic acid and substitution with hydroxypyridine.

After 2 days at 80°C, the reaction was no longer purple, indicating that all the oxidizing agent had been consumed. Workup by filtration, acidification, and Soxlet extraction yielded a moderate amount of a yellow-white solid. ^1H NMR of this solid in D_2O showed a peak at 8.37 ppm as well as several very small unidentified peaks in the Ar-CH_3 region.

An attempt to convert this material to an iron phthalocyanine complex via the method of Busch[15] yielded no green solid as would be expected. The oxidation of the trimethyl compound might have been incomplete. Attempted oxidation of this dinitro species seemed to hasten the decomposition of the $KMnO_4$ as compared to the oxidation of similar compounds, such as the bromo-trimethylbenzene.

4-Hydroxypyridine Substitution of 3,5-Dinitro-1,2,4-Trimethylbenzene. As another approach to the desired phthalocyanine, we first tried a nucleophilic substitution on the 3,5-dinitro-1,2,4-trimethylbenzene before attempting to generate the triacid via oxidation[6] (Figure 23). The dinitro-trimethyl compound was heated in DMSO with 2 equivalents of 4-hydroxypyridine, which caused the color to change from yellow to brown. After extraction with CH_2Cl_2 and chromatography on silica, a brown solid was obtained, which resembled the mono-substituted compound ^1H NMR (chemical shift, integration). The solid obtained had an approximately 33% yield.

Attempted Oxidation of 5-Nitro-3-Oxypyridino-1,2,4-Trimethylbenzene. The nitro-oxypyridinotrimethylbenzene was mixed with 7.5 equivalents of $KMnO_4$ (and Na_2CO_3) in water. Within 1 h at 90°C, the purple color had disappeared. A typical workup was carried out (i.e. acidification with HCl and extraction with CH_2Cl_2). The NMR spectra of both the water-soluble and the CH_2Cl_2-soluble fractions showed many peaks in the regions for Ar-H (7-9 ppm) and Ar-CH_3 (2-3 ppm), indicating either incomplete oxidation and/or decomposition of the starting material. Apparently, the starting material caused the rapid decomposition of the $KMnO_4$.

We decided to change directions and attempt the displacement reaction from a brominated aromatic instead of the nitroaromatic.

Bromination of 1,2,4-Trimethylbenzene. A bromo-1,2,4-trimethylbenzene should be almost as good as a nitro derivative for our goal of coupling to 4-hydroxypyridine. Bromination of 1,2,4-trimethylbenzene using 0.88 equivalent of bromine in benzene, catalyzed by a small amount of iron filings, led to the formation of a single brominated product. This product was isolated as a white, crystalline solid with a 67% yield. The NMR spectra was consistent with 5-bromo-1,2,4-trimethylbenzene. The reaction was repeated on a large scale.

The first attempt was to substitute the bromotrimethylbenzene prior to oxidation to the triacid, as shown in Figure 24.

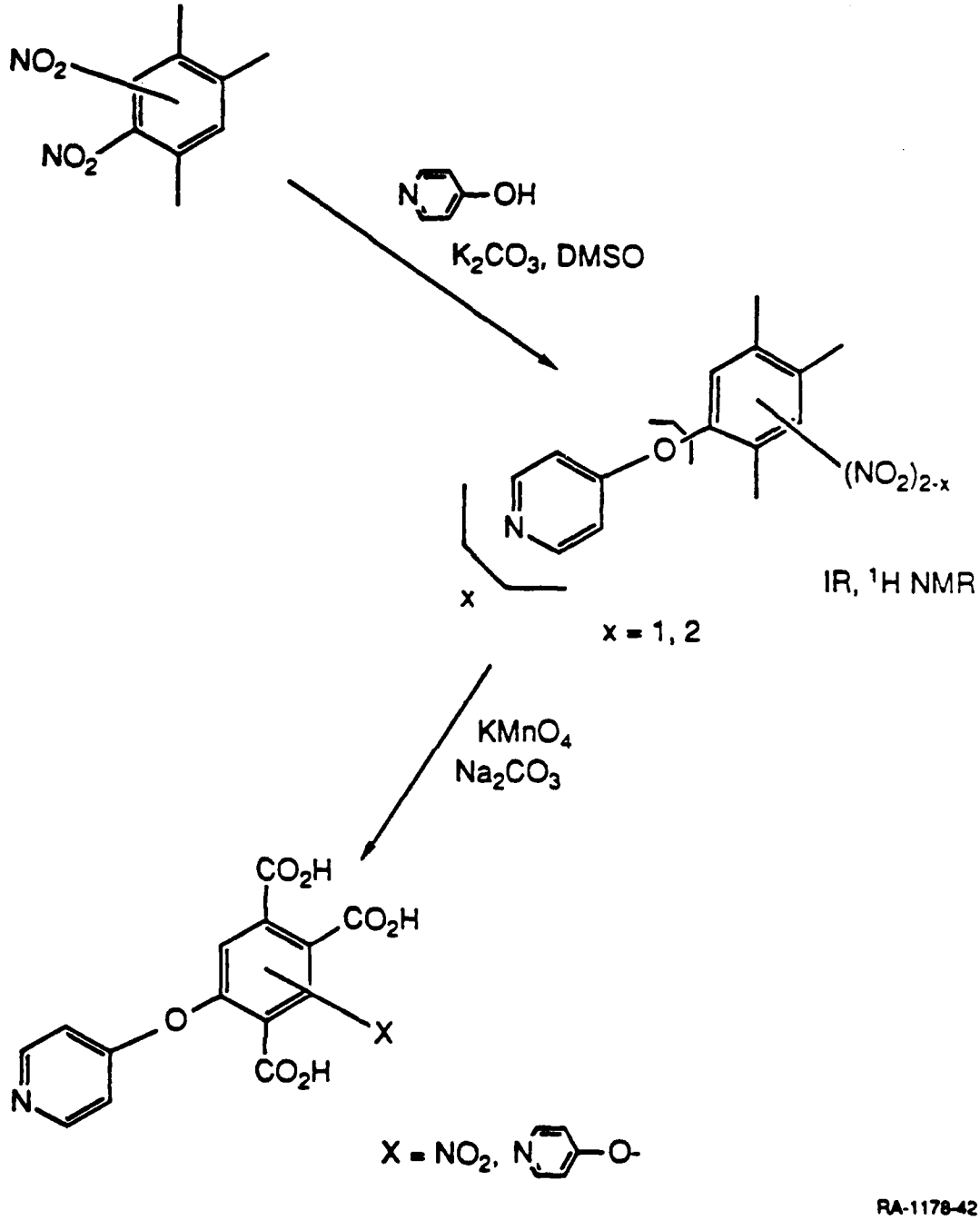

Figure 23. Substitution of the dinitrotrimethylbenzene to give the 5-nitro-3-oxypyridine 1,2,4-trimethylbenzene followed by oxidation.

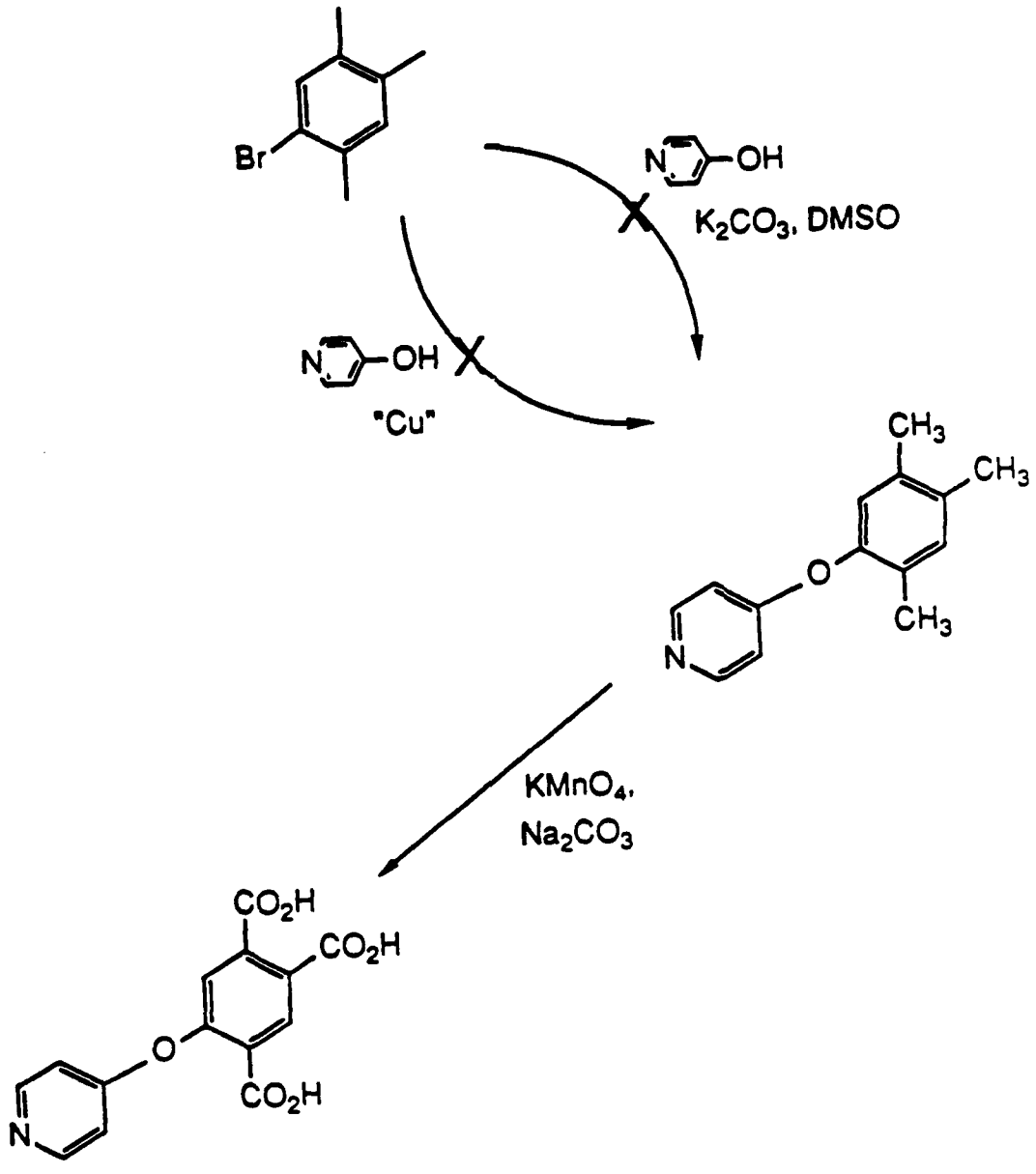

RA-1178-43

Figure 24. Substitution of 5-bromotrimethylbenzene followed by oxidation to the corresponding triacid.

Attempted Coupling of Bromotrimethylbenzene with 4-Hydroxypyridine. One method for effecting nucleophilic substitution on an acyl halide is by using copper reagents. This approach is known as the Ullmann Ether Synthesis.[2] We wanted to employ this type of reaction to couple the 4-hydroxypyridine to either the iron tetrabromo-tetraamidophthalocyanine (Br_4FeTAPC) or one of its precursors.

In one variation of the reaction, the 5-bromo-1,2,4-trimethylbenzene was combined with the hydroxypyridine, K_2CO_3, and Cu_2O in collidine under nitrogen. This pale tan-yellow supernatant and purple insoluble Cu_2O mixture was refluxed for 3 days, giving a black supernatant and a black precipitate. After workup, only a brown liquid was obtained, the NMR of which showed to contain collidine and starting material as the only identifiable species. The conditions (170°C) might have been too harsh. The reaction was not pursued because of the negative results from the attempted oxidation of a similar product, the hydroxypyridine-substituted nitrotrimethylbenzene. We decided to pursue oxidation of the bromotrimethylbenzene prior to substitution as an alternative as shown in Figure 25.

Oxidation of Bromotrimethylbenzene. To form the bromo-substituted phthalocyanine and effect substitution, we needed to synthesize the corresponding triacid compound. We synthesized it by oxidizing approximately 3 g of the 5-bromo-1,2,4-trimethylbenzene with $KMnO_4/Na_2CO_3$. The reaction proceeded over several days to yield 1.3 g (approximately 40%) of the crude product. The yield was reduced in part because some of the starting material had sublimed into the condenser. Soxlet extraction of the crude material with acetone was necessary to obtain appreciable amounts of product. The compound was soluble in water and only slightly soluble in acetone and ether.

Attempts to scale up the reaction (i.e., to 10 g of starting material) were only partially successful. Five ml of benzene per 200 ml of H_2O were used to reflux and wash sublimed starting material back into the reaction. However, yields inevitably dropped to approximately 10% after extraction.

Synthesis of Tetrabromotetraamido-Phthalocyanine (Br_4FeTAPC). The 5-bromo-1,2,4-tricarboxybenzoic acid was converted to the tetrabromo phthalocyanine (as the tetraamide).[15] After 20 h heating in nitrobenzene, an olive-green powder was obtained after filtration and washing with methanol and water (approximately 43% yield). This powder was not characterized before further reaction (see Figure 26).

Reaction of Tetrabromo-FeTAPC with Copper Phenoxide. Another variation of the Ullmann Ether Synthesis employs copper alkoxides instead of an alcohol and base.[21] The 4-oxypyridine copper species was prepared in situ by reacting n-BuLi with 4-hydroxypyridine to form the lithium alkoxide and then adding CuCl all under nitrogen. (The CuCl was first purified by washing with sulfuric then sulfurous acids.) To this beige mixture was added the Br_4FeTAPC in pyridine. The reaction quickly turned

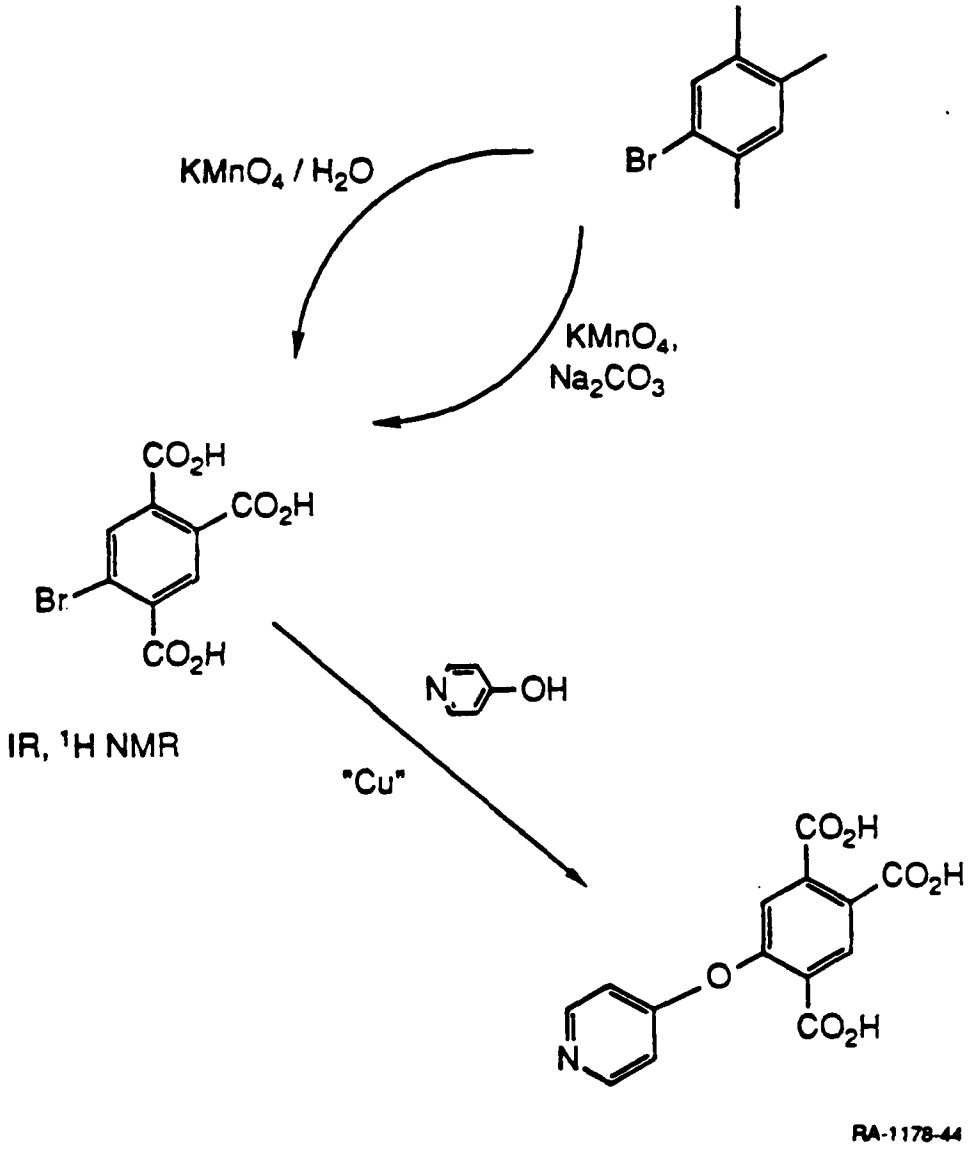

Figure 25. Oxidation of 5-bromo-1,2,4-trimethylbenzene followed by substitution with hydroxypyridine.

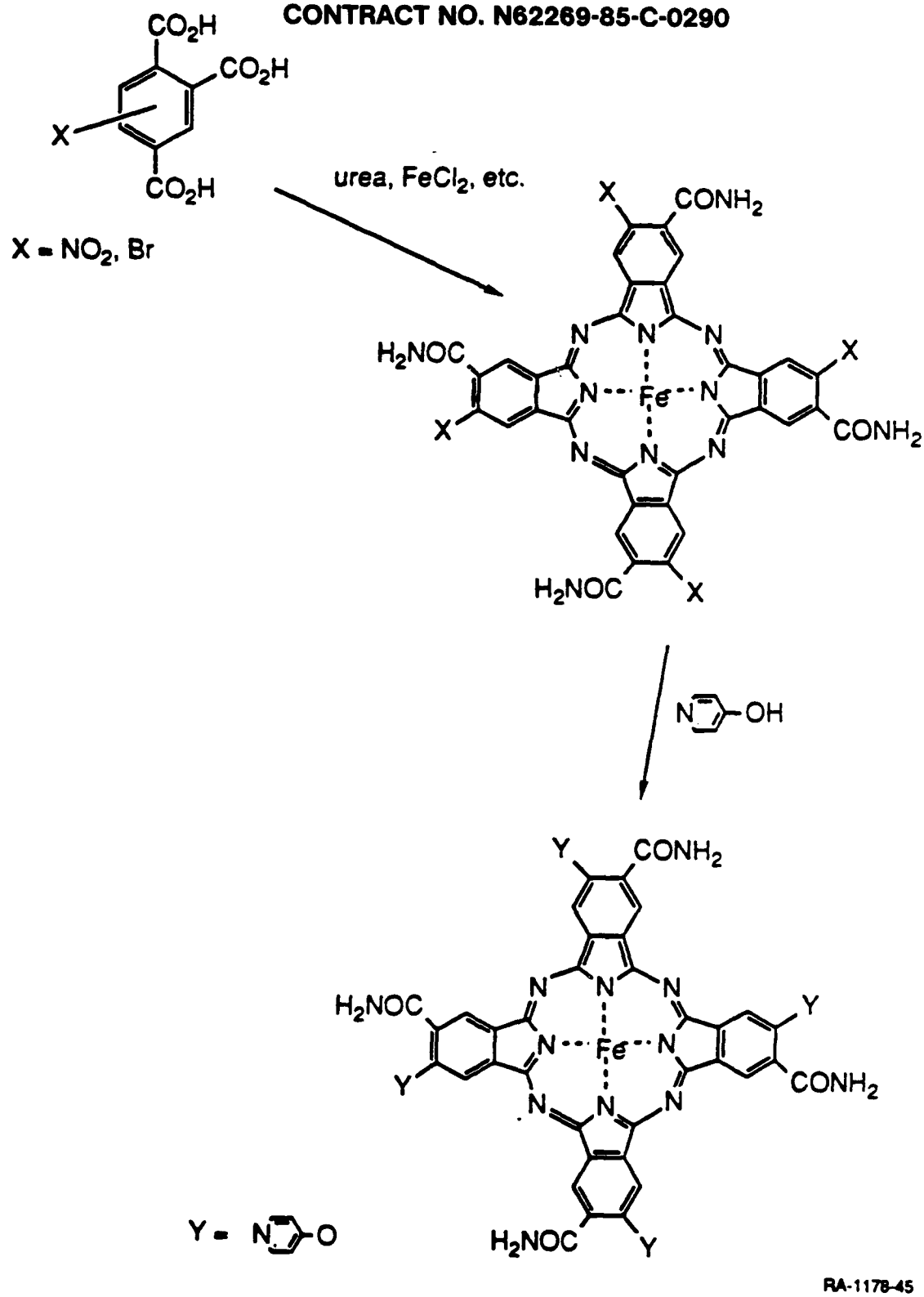

Figure 26. Conversion of substituted tribenzoic acid tetramido tetrabromophthalocyanine (or tetranitro) followed by substitution of the bromide (or nitro).

a very dark grey and after 17 h a green solid could again be separated from the reaction by filtration (approximately 85% yield). Attempts to convert the green solid to the tetracarboxylic acid by stirring at 90°C in 1 N NaOH produced a dark brown solid with a lower yield (approximately 60%).

This synthesis is a very promising result. The fact that we could isolate the tetraamidophthalocyanine with appropriate substitution to fill the void is promising. Unfortunately, we need more time to work on the conversion of the amidophthalocyanine to the acid form and to develop the polymerization of this substituted phthalocyanine to give the void-filled polymers.

Corrosion Studies

Only the first attempt at filling the void reached a stage for corrosion studies and that showed no improvement over the nonvoid-filled polymers (Figure 7). Therefore, we believe that void filling has not taken place when we attempted derivatization of the polymer-coated metal sample.

CONCLUSIONS

The work performed with phthalocyanines has shown that water-soluble phthalocyanines are not good as acid corrosion inhibitors. However, we have shown that some water-insoluble phthalocyanines such as Fe(III) TCPC when polymerized on a steel surface gave a reasonably high corrosion inhibition efficiency of 82%. This efficiency was obtained with a single coating after a single heat treatment at 450°C. Other polyphthalocyanines containing different metal ion centers such as Co(II), Si(IV), Zn(II), and Cr(III) gave even lower inhibition efficiencies ranging from 52% to 68%. Thus, among the polyphthalocyanines studied so far, poly-Fe(III) TCPC appears to be the best material as a corrosion-inhibiting coating. We believe that its inhibition efficiency can be further improved by having multiple coatings instead of a single coating.

Long alkyl chain substituted phthalocyanines appear to be extremely promising as corrosion-inhibiting coating materials. As an example, Fe(III) TCAUPC containing four ten-carbon alkyl chains (Figure 4) gave an inhibition efficiency of 88% while Zn(II) TCAUPC having the same organic structure gave a corrosion inhibition efficiency of 87% for steel in 1 N NaCl at pH = 2. Our results show that both the length of the alkyl chain and the nature of the central metal ion are important in providing higher inhibition efficiencies. Si(IV) TCAUPC having a ten-carbon alkyl chain gave a corrosion inhibition efficiency of 66%, which is much lower than its Fe(III) counterpart, which gave a corrosion inhibition efficiency of 88%.

The effect of alkyl chain length on the inhibition efficiency is seen when one compares the results obtained with Fe(III) TCAUPC and Fe(III) TCACPC where the former is the ten-carbon chain analog, which has an inhibition efficiency of 88% whereas the latter is the five-carbon chain analog, which has an inhibition efficiency of 84%. This effect is further proven when one compares Co(II) TCAUPC (ten-carbon chain) with Co(II) TCACPC (five-carbon chain) in which case the inhibition efficiencies are ~84% and 65% respectively.

Increasing the substituent alkyl chain length beyond ten and working with either Fe(III) or Zn(II) centered phthalocyanines is thus expected to result in inhibition efficiences much greater than 88%. Another area that should be explored is to have long alkyl chain containing phthalocyanines with silane end groups. They should, in principle, provide much higher corrosion inhibition efficiencies because of their ability to strongly anchor onto metal surfaces.

Our data also conclusively prove that phthalocyanines having long alkyl chains can drastically increase the film-forming ability of the

inhibitor because of Van der Waals type of interactions. These interactions can be enhanced by further increasing the length of the carbon chain and achieving inhibition efficiencies greater than 88%. These inhibitors have a unique advantage in that they only require a relatively low temperature heat treatment of 100-110°C.

Our preliminary attempts to develop a low void fraction phthalocyanine gave inhibition efficiencies of 77% for steel in 1% NaCl (pH = 2) solution. We believe that this low efficiency is due to the poor adherence of the polyphthalocyanine on the metal when the polymer present on the metal surface is derivatized. We changed our approach during the second year of the project by attempting to first synthesize the appropriately derivatized monomer and then polymerize it on the metal surface by using the same heat treatment that we have used previously. We have been able to synthesize the tetraamidophthalocyanine with appropriate substitution to fill the void. However, further work is needed on the conversion of the amidophthalocyanine to the acid form and the development of the polymerization method to give the void-filled polymer.

The work to date on aluminum-7075 alloy shows that phthalocyanines or polyphthalocyanines are not very effective in inhibiting corrosion of aluminum-7075 alloy in 1% NaCl (pH = 2) solution. We therefore adopted a different approach to inhibit corrosion of aluminum-7075 alloy by first etching its surface to obtain a porous oxide film and then attaching the hydrophillic end of a silane surfactant on to the hydrophillic aluminum oxide surface. This approach resulted in a strongly hydrophobic aluminum surface with the long-chain alkyl groups protruding from the surface. The inhibition efficiency obtained was 86%. We believe that higher efficiencies are possible by depositing phthalocyanines on the now hydrophobic surface or by synthesizing long-chain phthalocyanines having trichlorosilane groups attached to the free end of the hydrocarbon chain. In either case we expect inhibitor efficiencies much higher than 86%.

Weight loss studies indicate that the poly Fe(III) TCPC coating remains intact with no weight loss over the period of time tested. No observable attack was found on the coating. However, the polyFe(III) TCPC coatings after a methanol rinse following the immersion in the phthalocyanine monomer became detached during weight loss experiments. Thus, we believe that methanol rinse step should be avoided to obtain a coating having good adhesion.

Both uncoated as well as silane- and phthalocyanine-treated aluminum-7075 alloy did not show any weight loss in an acid NaCl environment over the 2-week test. This fact indicates that the oxide film formed on the alloy provides adequate protection.

The work we performed with phthalocyanines has shown that high corrosion inhibition efficiencies of 88% for steel are achievable with phthalocyanines containing long chain aliphatic groups with a possible

goal of reaching 95-98% efficiency with another year's work. To our knowledge, this is the first time such high inhibition efficiencies have been achieved with macrocyclic inhibitors such as porphyrins or phthalocyanines. We believe that this finding opens up a whole new area of corrosion inhibitor research involving the synthesis and evaluation of electronically conducting monomeric and polymeric inhibitor coatings. We see a tremendous potential in this area of science, particularly because of the ability of the doped phthalocyanines to conduct electricity and their other unique properties (Table 10).

In addition, phthalocyanine coatings also have good lubricating properties because of their graphite like structure (Figure 27). Thus, we believe that these coatings can be used on moving components such as ball or roller bearings. To our knowledge, this study is the first exhaustive evaluation of electronically conducting corrosion inhibitor coatings.

Corrosion inhibitors conventionally used in the past generally form nonconducting films or coatings on the metal. Thus, although the coating protects the metal, it does so by sacrificing an important property of the metal surface, that is, the ability to use it as a conducting surface. However, our approach allows this important property of the metal to be maintained while protecting it from corrosion. Among some of the important applications of this property are the formation of EMI coatings and Faraday cages necessary for protecting sensitive electronic components and equipment from extraneous interfering electrical and electromagnetic noise when they are used in electrically or electromagnetically noisy environments such as industrial complexes, aircrafts, ships, and submarines. Among the last three applications, the most important will be those involving intelligence information gathering systems where increased signal-to-noise ratio is of paramount importance. In such applications the conducting polymeric coatings having corrosion inhibition properties can be used to filter the extraneous electrical noise.

Table 10

UNIQUE PROPERTIES OF PHTHALOCYANINE COATINGS

- Interact strongly with metal surfaces by chemisorption
- Strong adhesion
- Rigid planarity
- Large area coverage per molecule
- Have metallic character
- Provides a conducting surface
- Lubricity of the coatings
- Ability to obtain thin coatings
- Ease of forming a polymer
- Ability to achieve variable degree of inhibition by changing the central metal ion as well as the organic substituents.

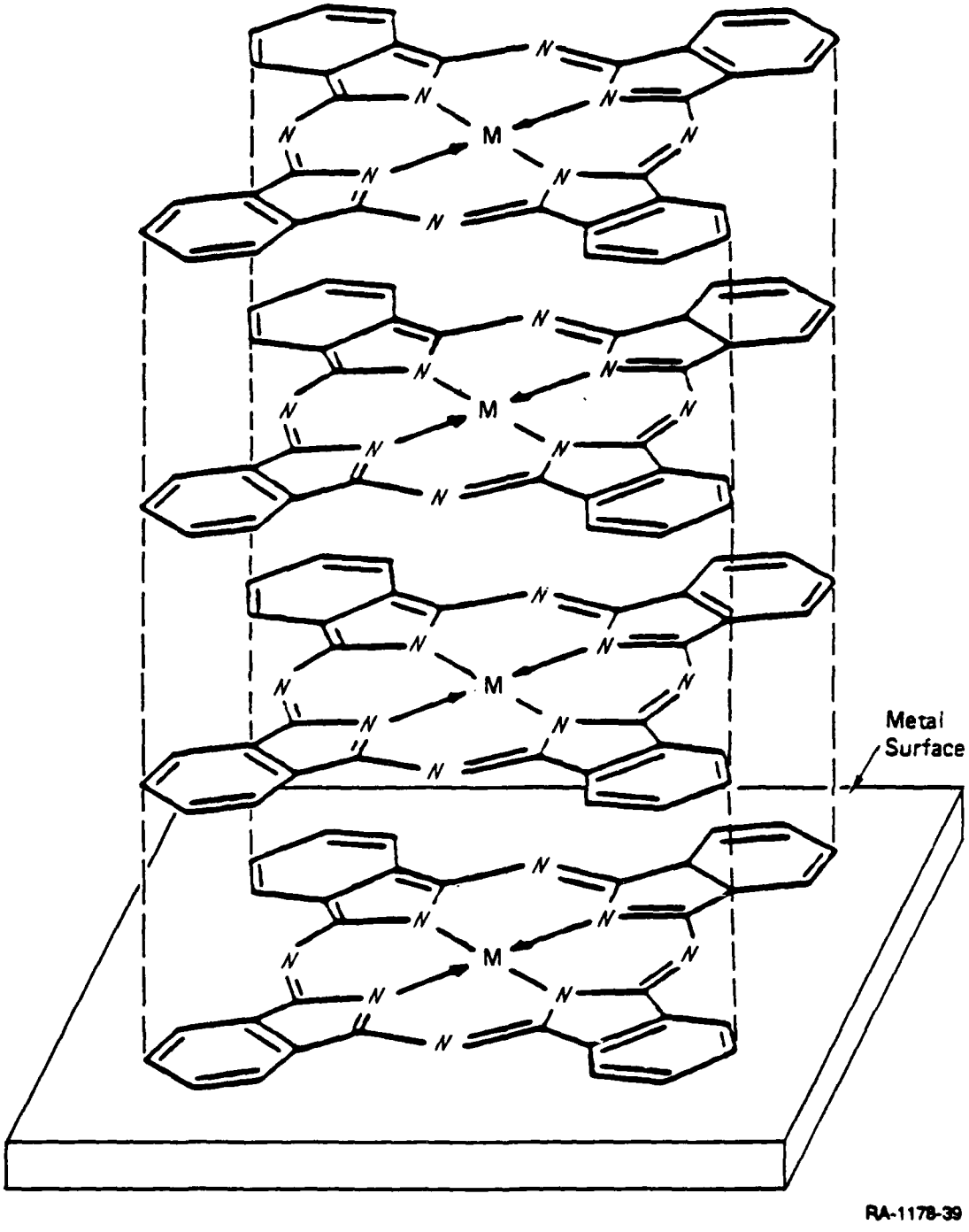

Figure 27. Assembly of metallophthalocyanines on a metal surface showing graphite-like layer-wise arrangement.

RECOMMENDATIONS

Because of the success we have had with the use of phthalocyanines as corrosion inhibitors, we recommend that this work be continued to enhance the inhibitor efficiencies from 88% to >95%. In addition, because phthalocyanines have good electronically conducting properties, good lubricating properties, and good thermal stability, we recommend that their multifunctional use should be explored and exploited in the areas of EMI coatings, ball and roller bearing coatings, and high-temperature conducting coatings. The major recommendations for future work in this area are listed below.

1. Initiate work on Mo(VI) TCPC, Pb(II) TCPC, In(III) TCPC, Ni(II) TCPC, and their long chain substituted counterparts (Figure 4) having more than ten carbon atoms in the alkyl chain. Increasing the length of the carbon chain will result in a high degree of Van der Waals interactions, thereby increasing the hydrophobicity of the coating. This work is a logical extension of the work we have done so far, where we have shown that both the nature of the central metal ion and the length of the alkyl chain are critical parameters for enhancing inhibition efficiency.

2. Explore the use of multiple coatings and other polymerization methodologies such as using UV treatment. In this case we propose to use vinyl substituted phthalocyanines as the monomer to obtain a polymer with a polyvinyl backbone with phthalocyanine pendant groups.

3. Initiate exploratory work to evaluate the potential use of phthalocyanines and polyphthalocyanines in EMI coatings. The silver powder impregnated polymer seals now used for this purpose cause severe galvanic corrosion at the joints. Therefore, we recommend exploring the possibility of using appropriately doped polyphthalocyanines and silver and aluminum based polyphthalocyanine conducting polymers to achieve contact resistances in the range of milliohms. We consider this to be an extremely promising area for future research.

4. Investigate the use of more effective end groups such as NH_2, NR_3, $SiCl_3$, and $Si(OR)_3$ in the long alkyl chains. These end groups are expected to anchor strongly onto metal surfaces, thereby providing better adhesion and improved corrosion inhibition. Another possibility is to have a silane end group in the alkyl chain and a quarternary ammonium group somewhere along the alkyl chain. This would provide additional corrosion

inhibition because of the synergistic action of the quarternary ammonium group.

5. Continue the work on synthesizing void-filled phthalocyanines (Figure 3) because we have come almost to the final stage of the synthesis. We have already synthesized the tetramidophthalocyanine, and we need time to convert this product to the acid form and subsequent polymerization.

During the project we have synthesized corrosion inhibiting coatings having metallic and lubricating properties that we believe is a unique development in the corrosion inhibiting coating technology. We believe that major development and applications of this technology will be seen in the next few years.

REFERENCES

1. K. Letts and R. Mackay, Inor. Chem. 14, 2293 (1975).

2. M. Zerner and M. Gouterman, Theoret. Chim. Acta 4, 44-63 (1966).

3. F. Longo, Report No. NADC-84167-60, Final Report Contract No. N6229-81-C-0278 (July 1984).

4. R. Charadlor, Paint Mfg. 6, 60 (1964).

5. K. Rajan, Natl. Intl. Serv., AD720384, U.S. Department of Commerce, Washington, DC (1970).

6. A. Snow and N. Jarvis, J. Am. Chem. Soc., 106, 4706 (1984).

7. B. Hoskins, S. Mason, and J. White, J.C.S. Chem. Com 554-595 (1969).

8. T. Kobayashi, F. Kurokawa, T. Ashida, N. Uyeda, and E. Suito, J. C. S. Chem. Comm. 1631-1632 (1971).

9. T. Kobayashi, T. Ashida, N. Uyeda, E. Suito, and M. Kakudo, Bull. Chem. Soc. Jpn. 44, 2095-2103 (1971).

10. B. Wheeler, G. Nagasubrananian, A. Bard, L. Schechtmen, D. Dinninny, and M. Kenney, J. Am. Chem. Soc. 106, 7404-7410 (1984).

11. K. Wynne, Inorg. Chem. 24, 1339-1343 (1985).

12. T. Marks, Science 227, 881-889 (1985).

13. D. F. Evans, J. Chem. Soc., 2003 (1959)

14. P. Hambright and A. J. Bearden, in Porphyrins and Metalloporphyrins, K. M. Smith, Ed (Elsevier, 1975), p. 546.

15. J. H. Weber and D. H. Busch, Inorg. Chem. 4, 469 (1965).

16. J. H. Weber and D. H. Busch, Inorg. Chem. 4, 472 (1965).

17. F. H. Moser, in The Phthalocyanines, A. L. Thomas, Ed. (CRC Press, Inc. 1983), p. 168.

18. R. Farina, D. Halko, and J. Swinehart, J. Phys. Chem. 76, 2343 (1972).

19. H. Shirai, A. Maruyama, K. Kobayashi, and N. Hojo, Makromal. Chem., 181, 575 (1980)

20. B. N. Achar, G. M. Fohlen, and J. A. Parker, J. Polymer Sci., 21, 589 (1983).

21. M. Stern and A. L. Geary, J. Electrochem. Soc., 104, 56 (1957).

22. I. Epelboin, P. Morel, and H. Takenouti, J. Electrochem. Soc., 118, 1282 (1971).

23. I. Epelboin, M. Keddam, and H. Takenouti, 3rd European Symposium on Corrosion Inhibitors, Ferrara, Italy (1970), p. 237.

24. A. Caprini, I. Epelboin, P. Morel, and H. Takenouti, 4th European Symposium on Corrosion Inhibitors, Ferrara, Italy (1975), p. 517.

DISTRIBUTION LIST (continued)

No. of Copies

Dr. Bryan E. Wilde 1
Fontana Corrosion Center
The Ohio State University
Columbus, OH 43210

Chief, Materials & Processes 1
Grumman Aerospace
Bethpage, LI, NY 11714

Chief, Materials & Processes 1
Vought Corporation
P.O. Box 5907
Dallas, TX 75222

Chief, Materials & Processes 1
Rockwell International
4300 East Fifth Street
Columbus, OH 43216

Chief, Materials & Processes 1
Boeing Aerospace
P.O. Box 3707
Seattle, WA 98124

Chief, Materials & Processes 1
Lockheed Aircraft Corporation
2555 North Hollywood Way
Burbank, CA 91503

Chief, Materials & Processes 1
McDonald Douglas Corporation
P.O. Box 516
Saint Louis, MO 63166

Cleveland Pneumatic Corporation 1
3781 East 77th Street
Cleveland, OH 44105

Center for Naval Analyses 1
4401 Fort Ave.
P.O. Box 16268
Alexandria, VA 22302-0268

Naval Air Development Center 12
Warminster, PA. 18974-5000
(2 copies to Code 8131)
(10 copies to Code 6062: ATTN: Dr. Vinod Agarwala)

DISTRIBUTION LIST (continued)

No. of Copies

Dr. Glenn E. Stoner 1
Dept. of Materials Science & Engineering
University of Virginia
Charlottesville, VA 22901

Dr. Barry C. Syrett 1
Electric Power Research Institute
3412 Highview Avenue
P.O. Box 10412
Palo Alto, CA 94303

Dr. A. Thompson 1
Dept. of Metallurgical Engineering &
Material Science
Carnegie Mellon University
Pittsburg, PA 15212

Dr. H. Townsend 1
Homer Research Laboratories
Bethlehem Steel Corporation
Bethlehem, PA 18016

Dr. A. R. Troiano 1
Dept of Metallurgy & Materials Science
Case Western Reserve University
Cleveland, OH 44106

Dr. Gilbert Ugiansky 1
President
Cortest Engineering Services
15200 Shady Grove Raod
Rockville, MD 208500

Dr. S.K. Varma 1
IIT Research Institute
10 West 35th Street
Chicago, IL 60616

Prof. Elis Verink 1
Dept. of Materials Science & Engineering
University of Florida
Gainsville, FL 32611

Dr. Robert Wei 1
327 Sinclair Laboratory
Lehigh University
Bethlehem, PA 18015

DISTRIBUTION LIST (continued)

No. of Copies

Dr. M. R. Louthan 2
Materials Engineering Dept.
Virginia Polytechnic Institute
Blacksburg, VA 24061

Dr. Digby D. Macdonald 1
SRI International
333 Ravenswood Avenue
Menlo Park, CA 94025

Dr. Florian Mansfeld 1
VHE714
Dept of Materials Science
University of Southern California
Los Angeles,CA 90009-0241

Dr. C McMahon,LRSM 1
University of Pennsylvania
Philadelphia, PA 19104

Dr. Joe H. Payer 1
Dept. of Metallurgy & Materials Science
Case Western Reserve University
10900 Euclid Avenue
Cleveland, OH 44106

Dr. Joseph Pickens 1
Martin Marietta Laboratory
1450 South Rolling Road
Baltimore, MD 21227

Dr. Howard W. Pickering 1
Penn State University
209 Steible Building
University Park, PA 16802

Dr. L. Raymond 1
L. Raymond Associates
P.O. Box 7925
Newport Beach, CA 92658-7925

Mr. Jules F. Senske 1
ARDC Bldg 355
Dover, NJ 07801

Mr. Paul Shaw 1
Grumman Aircraft Systems
Bethpage, NY 11714-3582

DISTRIBUTION LIST (continued)

No. of Copies

Dr. D. J. Duquette 1
Rensselaer Polytechnic Institute
Materials engineering Department
Troy, NY 12181

Dr. Robert P. Frankenthal 1
A T & T Bell Laboratories
Room 10-352
600 Mountain Avenue
Murray Hill, NJ 07974

Dr. John Green 1
Martin Marietta Laboratories
1450 South Rolling Road
Baltimore, MD 21227

Dr. Norbert D. Greene (U-136) 1
University of Connecticut
Storrs, CT 06268

Dr. Samsom S. Hettiarachchi 1
SRI International
333 Ravenswood Avenue
Menlo Park, CA 94025

Dr. M. W. Kendig 1
Rockwell International Science Center
1049 Camino Dos Rios, P.O.Box 1085
Thousand Oaks, CA 91360

Dr. Michael J. Koczak 1
Dept of Materials Engineering
Drexel University
Philadelphia, PA 10104

Drs. J. Kruger & P. J. Moran 1
Dept of Materials Science & Engineering
Johns Hopkins University
Baltimore, MD 21218

Dr. H. Leidheiser, Jr. 1
Center for Coatings & Surface Research
Lehigh University
Bethlehem, PA 18015

DISTRIBUTION LIST (continued)

No. of Copies

Dr. Robert Reeber 1
U.S.Army Research Office
P.O. Box 12211
Research Triangle Park, NC27709

Dr. J. Wells 1
SLCMT-MCZ
Materials Technology Laboratory
Weatertown, MA 02172-0001

Belvoir Research, Development &
Engineering Center 1
Mr. Dario A. Emeric (STRBE-VC)
Fort Belvoir, VA 22060-5606

Dr. Phillip Parrish 1
Defense Advanced Research Projects Agency
1400 Wilson Blvd. (6th Floor)
Arlington, VA 22209

Dr. Charles G. Interrante 1
Corrosion Group, Metallurgy Div.
National Bureau of Standards
Washington, DC 20234

Dr. E. N. Pugh 1
Room B254, Bldg. 223
National Bureau of Standards
Washington, DC 20234

Defense Technical Information Center 2
Attn: DTIC-DDA-1
Cameron Station, Bldg. 5
Alexandria, VA 22314

Dr. Lionel J. Bailin 1
Lockheed Missile & Space Co. Inc.
3251 Hanover Street
Palo Alto, CA 94303

Dr. Theodore R. Beck 1
Electrochemical Technology Corp.
3935 Leary Way N.W.
Seattle, WA 98109

DISTRIBUTION LIST (continued)

No. of Copies

Mr. J. Hall 1
Code G53, Materials Group
Naval Surface Warfare Center
Dahlgren, VA22448

Mr. A. J. D'Orazio 1
Code PE-72
Naval Air Propulsion Center
Trenton, NJ 08628

Mr. James Jenkins 1
Code 152
Naval Civil Engineering Laboratory
Fort Hueneme, CA 93043

Dr. Richard W.Drisco 1
Code 152
Naval Civil Engineering Laboratory
Port Hueneme, CA 93043

Dr. Jeff Perkins 1
Code 69
Naval Post Graduate School
Monterey, CA 93943

Dr. Alan Rosenstein 1
U.S. Air Force
Office of Scientific Research
Bolling AFB, Washington, DC 20332

Mr. Bennie Cohen 1
AFWAL/MLSA
Wright Patterson A.F.B., OH 45433

Mr. R. Kinsey 1
MMEMC
Air Force Logistics Center
Warner-Robins AFB
Warner, GA 31908

Mr. Milton Levy 1
SLCMT-M
U.S. Army Materials & Mechanics Research Center
Watertown, MA. 0272-0001

DISTRIBUTION LIST (continued)

No. of Copies

Mr. Anthony Corvelli 1
Code 36621
Naval Underwater Systems Center
Newport, RI 02841

Dr. B. Rath 1
Code 630
Naval Research Laboratory
Washington, DC 20375

Dr Edward McCafferty 1
Code 6314
Naval Research Laboratory
Washington, DC 20390

Mr. Dale A. Meyn 1
Code 6312
Naval Research Laboratory
Washington, DC 20375

Dr. R. Sutula 1
Code R33
Naval Surface Warfare Center
Silver Springs, MD 20910

Head, Materials Division 1
R & D Department
Naval Surface Weapons Center
Silver Springs, MD 20910

Dr. John Gudas 1
Code 2810
David Taylor Research Center
Annapolis, MD 21402

Mr. I. Kaplan 1
Code 0115
David Taylor Research Center
Annapolis, MD 21402-5067

Dr. R.G. Kasper 1
Code 4493
Engineering Mechanics Division
Naval Underwater Systems Center
New London, CT 06320

DISTRIBUTION LIST (continued)

No. of Copies

Commanding Officer 1
Naval Aviation Depot
Norfolk, VA 23511

Commanding Officer 1
Naval Aviation Depot
North Island
San Diego, CA 92135

Commanding Officer 1
Naval Aviation Depot
Pensacola, FL 32508

Commanding Officer 1
Naval Aviation Depot
Marine Corp Air Station
Cherry Point, NC 28533

Commander 1
Naval Air Force
U S Atlantic Fleet
Code 5281
Norfolk, VA 23511

Commander 1
Naval Air Force
U.S. Pacific Fleet
Attn: Code 7412
San Diego, CA 92135

Commander 1
Naval Sea Systems Command
Washington, DC 20362

Naval Weapons Center 1
Attn: Dr. R. Derr
Code 38
China Lake, CA 93555

Dr. James J. Carney 1
Naval Air Propulsion Center
PE-31 P.O. Box 7176
Trenton, NJ 08628